

NOVEL NANOCOMPOSITES FOR THE TREATMENT OF LUNG INFECTIONS

By

UDAY KUMAR CHINTAPULA

Submitted to the Graduate School of
The University of Texas at Arlington in partial fulfillment
of the requirements for the degree of
Doctor of Philosophy

Department of Bioengineering
University of Texas at Arlington

Supervising Committee:

Dr. Kytai T. Nguyen, Supervising Professor
Dr. He Dong, Co-supervising Professor
Dr. Jun Liao, Dissertation Committee Member
Dr. Michael R Roner, Dissertation Committee Member
Dr. Joseph Boll, Dissertation Committee Member

May 2022

Arlington, TX

ABSTRACT

Lung infections, especially lower respiratory tract infections and their associated pneumonias, are one of the leading causes of death, accounting for more than 4 million fatalities every year worldwide. Bacterial pathogens are involved in many lower respiratory tract infections including emerging antibiotic resistant respiratory pathogens such as methicillin-resistant staphylococcus aureus (MRSA). Current interventions for MRSA lung infections include systemic antibiotic treatments for an extended period leading to various side effects such as acute kidney injury, nephrotoxicity, and so on. To overcome these limitations, the goal of this dissertation research is to develop a drug delivery system, which includes pathogen-specific drug-loaded nanocomposites for targeting injured cells and ameliorating lung injury caused by these pathogens more effectively than conventional treatments. Specifically, non-invasive techniques such as inhalable formulations of our novel nanocomposites can increase patient compliance, reduce multiple doses, and improve therapeutic efficiency of potent drugs. To reach our goal, two specific aims were followed: (1) To synthesize and characterize nanocomposites comprised of PLGA-based nanoparticles with nanofiber coating as an enhanced drug delivery platform, and (2) To develop and evaluate antimicrobial-loaded nanocomposites for treatment of MRSA lung infections. The main innovative aspects of our system are that it effectively reduces bacterial infections via a unique design strategy of (1) FDA-approved PLGA material-based nanoparticles for loading of antimicrobials drugs to inhibit bacteria growth, (2) Enhanced cellular uptake of our system provided by nanofiber coating of nanoparticles, and (3) Higher bioavailability of drugs at the infected area by employing an inhalable method to deliver the nanocomposites directly to the lung infection tissues. Our results with novel nanocomposites in infected lung epithelial cells show

higher uptake compared to nanoparticles. In addition, antimicrobial-loaded nanocomposites significantly reduce the pathogen burden in cells compared to free drug and microbial-loaded nanoparticles. These results suggest the potential of our novel nanocomposites to treat lung infections via a more targeted approach with enhancement in drug delivery. These results indicate that our research might have a significant impact in human health in the future as it might bring an improvement in the treatment of MRSA lung infections by saving many lives and providing efficient therapeutic strategies for lung infections.

Copyright © by Uday Kumar Chintapula

2022

All Rights Reserved

The University of Texas at Arlington

Acknowledgements

Many people are involved in this successful journey to complete my PhD. Above all, I would like to thank my family for being an example by showing how hard work and perseverance is the key to succeed in whatever journey you undertake. A special shoutout to my elder brother Mr. Kranthi Chintapula, who stood by me through thick and thin. I would like to dedicate this thesis to my family. Also, to my fiancé Swarna, for being patient and supportive of my PhD journey.

I sincerely thank all my committee members: to Dr. He Dong for her full support in this wonderful collaboration, to Dr. Jun Liao for his warm-hearted support, to Dr. Roner for his guidance in my bacteria experiments, and to Dr. Joseph Boll and Dr. Hao Xu for taking time out of their busy schedule to review my work and give valuable advice to improve my thesis research. To my dissertation supervisor Dr. Kytai Nguyen, who has always given me her full support to explore different avenues in my research and is an excellent mentor throughout my PhD journey, I would never become the professional I am today without you, my academic mother. She has helped me to grow both as a person and as an independent researcher. I would also like to express my gratitude to the Department of Bioengineering for its support through various funding sources. In addition, I am thankful to the wonderful team members of the nanomedicine and drug delivery laboratory, who have helped me to learn and grow. Lastly, I give my appreciation to all other friends and family, who have supported me through my journey.

May 4th, 2022

TABLE OF CONTENTS

Abstract.....	ii
Copyright.....	iv
Acknowledgements.....	v
List of Figures.....	ix
List of Tables.....	x
Chapter 1: Introduction.....	1
1.1 Lung physiology and common lung infections.....	1
1.1.1 Pulmonary Physiology.....	1
1.1.2 Common Lung Infections.....	2
1.1.3 Bacterial Lung Infections.....	3
1.2 Current Treatments for <i>S. aureus</i> Lung Infections and Their Shortcomings	5
1.3 Nanomedicine Interventions in the Treatment of Lung Infections	7
1.3.1 Type of NPs.....	9
1.3.1.1 <i>Micelles</i>	9
1.3.1.2 <i>Liposomes</i>	10
1.3.1.3 <i>Polymer nanoparticles</i>	11
1.3.2 Peptide Coated Nanoparticles.....	12
1.3.3 Cellular Uptake Mechanisms of NPs in Infected cells.....	13
1.4 Design consideration of drug delivery systems targeting lung infection.....	15
1.5 Overview of dissertation project.....	16
1.5.1 Objectives.....	16
1.5.2 Specific aims.....	17
1.5.3 Innovative aspects.....	17
1.5.4 Successful outcomes.....	18
Chapter 2: Synthesis and Characterization of Novel Nanocomposites for Enhanced Pulmonary Drug Delivery.....	19
2.1 Introduction.....	19
2.2 Methods.....	20
2.2.1 Materials used.....	20
2.2.2 Synthesis of Nanocomposites.....	21
2.2.3 Characterization of Nanocomposites.....	22

2.2.3.1 DLS measurements.....	22
2.2.3.2 Fluorescent microscopy.....	22
2.2.3.3 FTIR of nanocomposites.....	23
2.2.3.4 Binding kinetics of nanofibers to nanoparticles.....	23
2.2.4 Cytocompatibility of Nanocomposites.....	23
2.2.5 Cellular uptake of Nanocomposites.....	24
2.2.6 Mucus Permeation Study.....	25
2.2.7 In vitro Nebulization.....	26
2.2.8 Nanocomposite Cellular Uptake Mechanism Study.....	27
2.2.9 Effects of Nanocomposite Freeze-Drying.....	27
2.2.10 Nanofiber Coated NPs vs. HIV TAT Peptide Coated NPs.....	28
2.2.11 Time-Dependent Uptake of Nanocomposites.....	28
2.2.12 Statistical Analysis.....	28
2.3 Results and discussions.....	29
2.3.1 Characterization of Nanocomposites.....	29
2.3.2 In vitro Evaluation of Nanocomposites.....	31
2.3.3 Enhanced Cell Uptake Ability of Nanocomposites.....	33
2.3.4 Permeation of Nanocomposites.....	35
2.3.5 Uptake Mechanism of Nanocomposites.....	37
2.3.6 Translative Potential of Nanocomposites.....	39
2.4 Conclusion.....	40

Chapter 3: Antimicrobial Nanocomposites for the Treatment of Antibiotic Resistant MRSA

Lung Infections.....	42
3.1 Introduction.....	42
3.2 Methods.....	44
3.2.1 Materials.....	43
3.2.2 Synthesis of Antimicrobial Nanoparticles.....	43
3.2.3 Synthesis of Antimicrobial Nanocomposites (AMNCs).....	44
3.2.4 Characterization of Antimicrobial Nanoparticles.....	45
3.2.5 Cytocompatibility of AMNCs.....	46
3.2.6 Cell Uptake of NCs in Infected Cells.....	46
3.2.7 Antimicrobial Properties of Antibiotic Loaded Nanoparticles.....	47
3.2.7.1 Minimum inhibitory concentration (MIC) assay.....	47
3.2.7.2 Zone of Inhibition.....	47
3.2.8 Intracellular Killing efficiency of AMNCs.....	48
3.2.9 Nebulization of AMNCs.....	48
3.2.10 In vivo Biodistribution of Nanocomposite.....	49
3.3 Results and discussions.....	50
3.3.1 Synthesis and Characterization of AMNCs.....	50
3.3.2 Cytocompatibility of AMNCs.....	52
3.3.3 In vitro Evaluation of AMNCs Uptake in Infected Cells.....	51

3.3.4 Antimicrobial Properties of Vancomycin Loaded Nanoparticles.....	53
3.3.5 Intracellular MRSA Killing Using AMNC.....	55
3.3.8 <i>In vivo</i> Biodistribution of AMNCs.....	57
3.4 Conclusion.....	60
Chapter 4: Conclusions and Future Outlook.....	62
4.1 Conclusions.....	62
4.2 Limitations.....	63
4.3 Outlook.....	63
References.....	65
Biographical information.....	71

LIST OF FIGURES

Figure 1.1: Schematic of Lung Infection by Region.....	4
Figure 1.2: Current scenario for management of antimicrobial resistance.....	7
Figure 2.1: Schematic of nanocomposite synthesis.....	29
Figure 2.2: Characterization of nanocomposites.....	31
Figure 2.3: Cytocompatibility of nanocomposites.....	32
Figure 2.4: Cellular Uptake of Nanocomposites.....	33
Figure 2.5: Time dependent uptake of nanocomposites.....	34
Figure 2.6: Confocal Imaging of Internalized Nanocomposites in AT1 cells.....	35
Figure 2.7: Mucus Permeation Study.....	36
Figure 2.8. Cell Uptake Mechanism Study.....	37
Figure 2.9: Cell Uptake of Nanocomposites at Low Temperatures.....	38
Figure 2.10: Translative Potential of Nanocomposites.....	40
Figure 3.1: Schematic of AMNC Pulmonary Delivery and Inhibition of <i>S. aureus</i>	50
Figure 3.2: Characterization of AMNCs.....	51
Figure 3.3: Cytocompatibility of AMNCs.....	52
Figure 3.4: AMNC cell uptake in MRSA infected AT1 cells.....	54
Figure 3.5: Antimicrobial effects of Van-PLGA NPs.....	55
Figure 3.6: Intracellular MRSA Killing using AMNCs.....	56
Figure 3.7: AMNCs Nebulization to Inhibit Intracellular MRSA.....	57
Figure 3.8: Setup for Inhalation Delivery of Nebulized ICG-PLGA NPs and AMNCs in Mice.....	58
Figure 3.9: Biodistribution and H&E Staining of Lung Tissue for PLGA NPs and nanocomposites treatment via nebulization in mice.....	59
Figure 3.10: Biodistribution of Coumarin-6 dye loaded AMNCs in mice lungs.....	60

LIST OF TABLES

Table 1.1: Types of nanoparticles for pulmonary drug delivery.....	9
Table 1.2: Different endocytosis mechanisms of nanoparticle uptake.....	13

Chapter 1

INTRODUCTION

1.1 Lung Physiology and Common Lung Infections

Lungs are one of the major organs in direct contact with the environment involving gas exchange. It is critical to understand the physiology of lungs due to their exposure to various particulates including disease causing agents like bacteria and viruses. Increases in lung infections due to several factors, including the rise of antibiotic resistance in bacteria and pandemic-able viruses, have led to much interest around pulmonary drug delivery and nanotherapeutics. Among various drug delivery approaches, inhalational drug delivery offers an attractive mode of treatment due to its direct localization to the lungs with the aid of the natural gas exchange process. The following sections will briefly outline lung infection treatment strategies, which form the focus of this thesis, improved nanotherapeutics, and will specify long term goals and specific aims of this research.

1.1.1 Pulmonary Physiology

Understanding the pulmonary physiology is particularly important in targeting drugs or drug carriers to treat lung infections. A detailed description of the physiology is beyond the scope for this section; therefore, the focus is given to the physiology of major barriers protecting the lungs from complications arising with pathologies like infections. Air flow begins at the upper neck and passes into the thorax and branches into the bronchi of each lung [1]. Bronchi are then branched out as bronchioles where they spread into a large cross-sectional area ending in gas exchange units consisting of respiratory bronchioles, alveolar ducts and alveoli [1]. The ‘mucocilliary blanket’ or area covered by the ciliated epithelium is involved in cleaning the lungs

from inhaled particles and pathogens deposited on airway linings by forming a barrier across the endothelium and generating mucus to trap particulates.

The alveolar surface area is covered with pulmonary capillaries, which consist of alveolar Type I cells adhered to endothelial cells involved in vascular and airway responses [2]. Alveolar epithelial cells consist of both Type I and Type II epithelial cells. Type I epithelial cells cover more than 95% of the alveolar surface, whereas Type II cells present in the alveoli secrete surfactant and serve as stem cells to be differentiated, and they replenish Type I cells [3, 4]. Any pathogenic insults leading to damage of these surfaces can be detrimental due to the slow proliferative response seen in alveolar epithelial cells [5]. Surfactant lining the AT1 cells consists of various lipids and proteins, which help to modulate immune activities during any injury [6]. ATI cells have been shown to be involved in innate immune responses, expressing Toll Like Receptors (TLRs) in response to the Lipopolysaccharide (LPS) stimulation and other pro-inflammatory cytokines including CXCL5 in pneumonia induced lungs of mice, establishing that AT1 cells did respond to bacteria and participate in the innate immune system [7, 8]. Taken together, lung epithelium helps to maintain lung homeostasis, especially serving as a barrier from leakage of blood components and responding to bacterial insults by participating in innate immune responses.

1.1.2 Common Lung Infections

Infections are quite common in poor countries among all age groups but are prominently seen in adults among wealthy countries. Regardless, lung infections make the top mode of infection in both poor and wealthy countries, suggesting a correlation between globalization and an increase in pathogens and their variants [9]. The recent COVID-19 pandemic and emerging antibiotic resistant bacterial infections such as MRSA, carbapenem-resistant enterobacteria, and other drug resistant bacteria show the threat from the rise of infectious agents. The US National

Institutes of Health (NIH) has spent more than \$287 million in 2004 for the treatment of infectious diseases [9]. The Global Burden of Diseases, Injuries, and Risk Factors (GBD), a 2016 study, which assessed cases, deaths, and aetiologies for a period of 26 years found that lower respiratory infection episodes were around 336 million [10]. Although there is a decreasing trend in lower respiratory cases among children, the global population average age is still increasing and has led to concerns with patient compliance of potent drug treatments and adverse drug reactions (ADRs). Lung infections are the largest cause of disease burden in the human population worldwide, with a loss of 103,000 disability-adjusted life years [11]. Overall, these statistics suggest that there is a need to develop better treatment strategies and drug delivery systems to reduce mortality and morbidity associated with lung infections.

1.1.3 Bacterial Infections

An estimated 4 million people die every year due to respiratory diseases [12]. In children under 5, pneumonia caused by various bacterial infections accounts for 1.3 million deaths annually. Pneumonia remains the leading cause for deaths related to infectious diseases in the United States. In 2005, an estimated cost of \$34 billion was incurred to the health care system from pneumonia and influenza lung infections [13]. According to the World Health Organization (WHO), antibiotic resistance in bacterial infections is one of the looming threats for global health, which can lead to higher medical costs with increased hospital stays and eventually increases mortality. Additionally, secondary bacterial infections are seen as a complication of respiratory viral diseases leading to increased co-morbidity [14, 15]. Lower respiratory bacterial infections are caused by various bacterial strains including *Streptococcus aureus* (*S. aureus*), *Streptococcus pneumoniae*, and *mycobacterium tuberculosis*, among others. Here we focus on common *S. aureus*

infections due to their increasing resistance to potent antibiotics and potential to become a global threat as listed by the WHO.

Hospital-acquired and community-acquired *S. aureus* lung infections are on the rise due to globalization and closed community living. *S. aureus* infections of the lower respiratory tract (**Figure 1.1**) lead to severe morbidity and mortality in patients [16]. *S. aureus* is an opportunistic

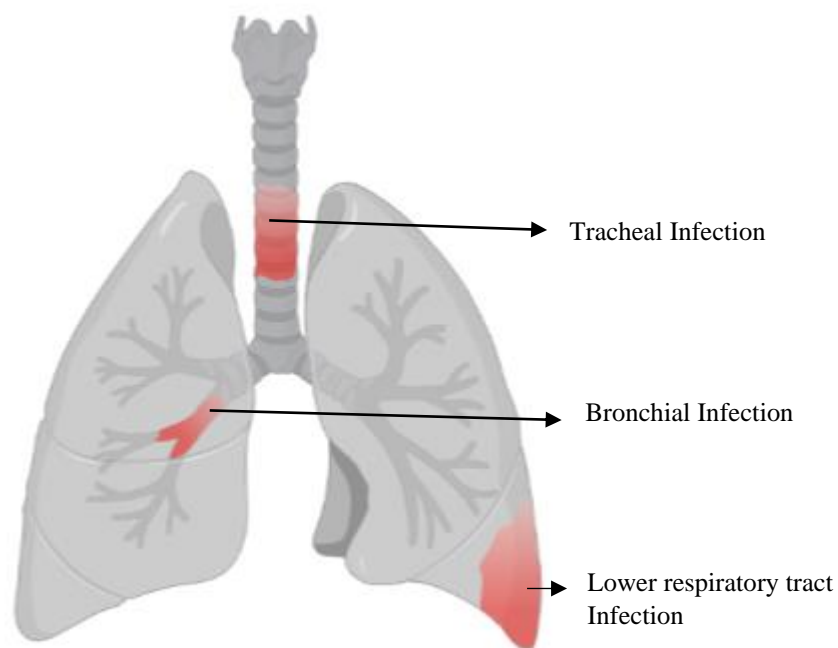


Figure 1.1 Schematic of lung infections by regions

pathogen, which can invade host cells such as macrophages, neutrophils, and even epithelial cells to result in apoptosis from *S. aureus* escape of endosomes [17-19]. *S. aureus* can persist for up to 4 days in the vacuoles of phagocytic cells before they escape into the cytoplasm, leading to cell lysis [20]. *S. aureus* immuno-activation through immune signaling via superantigens, protein A, *S. aureus* IgG binding protein (Sbi) and α -hemolysin may lead to a very high immune response resulting in ARDS condition in lungs [21]. *S. aureus* is the most common pathogen related to lung infections in Cystic Fibrosis (CF) patients in the early stages with an increase in prevalence from 0.1% in 1995 to 17.2% in 2005 [22]. *S. aureus* can also cause severe immune responses, with

airway epithelial cells having the primary immune signaling by recognition of surface components of the bacteria through pattern recognition receptors (toll-like receptors) to recruit immune cells [21]. Airway epithelial cells also respond to *S. aureus* infection via Interferon (IFN) signaling as seen with the incubation of epithelial cells with bacteria for more than 2 hours [23]. *S. aureus* infection causes an increase in immune cell transferring across the epithelial barrier increasing inflammation and conditions such as cytokine storms. Addressing the infection at the epithelial level can help restore the barrier and reduce further assault on the lungs. MRSA, an antibiotic resistant bacteria, can promote necrotizing pneumonia, septic shock, and respiratory failure; and MRSA infection treatments using the last resort drug Vancomycin are still insufficient with more than 50% mortality after treatment of severe cases [16]. Targeting alveolar epithelial cells (AT1), which cover ~95% of lung alveoli, to treat for MRSA can aid in restoring the epithelial barrier and alleviate lung injury.

1.2 Current Treatments for *S. aureus* Lung Infections and Their Shortcomings

Current interventions for lung infections include intravenous (IV) treatment of antibiotics to inhibit bacterial growth. Although various drug delivery strategies towards treating bacterial infections have been developed, their limitations include low compliance in older patients and side effects of antibiotics including acute kidney injury, cytotoxicity, and nephrotoxicity due to off-targeting. The sections below discuss the current treatment strategies to treat lung infections with a focus on MRSA, along with their drawbacks that need to be addressed.

Major treatment strategies in *S. aureus* lung infections or associated pneumonia include IV administration of antibiotics. Currently, antimicrobial therapy is mostly employed for severe lung infection/pneumonia caused by MRSA. Various antibiotics including Clindamycin, Nafcillin, Vancomycin, and Daptomycin are given intravenously every 4-12 hours, while Cephalexin,

Dicloxacillin and Linezolid are administered orally every 6-12 hours [24]. *S. aureus* infections mostly seen in influenza patients are treated with the Vancomycin drug via IV administration [24]. Vancomycin treatments have seen failures in Vancomycin-susceptible MRSA strains with an increase in the MICs from 2 µg/mL to 15-20 µg/mL evident in MRSA pneumonia treatment [25]. A 22% incidence of nephrotoxicity was observed in patients who received higher doses of Vancomycin or Vancomycin with a combination of drugs such as gentamycin sulfate [26]. Also, in patients aged ≥ 53 years, higher doses of Vancomycin increased the risk of ototoxicity significantly [27]. While most of the treatments for MRSA lung infections are given via IV, some antimicrobials given orally show insufficient outcomes to restore baseline lung functions, which can be from inaccurate dosages and drug resistance gained by bacteria from the current treatment regimen [28]. Hence, there is a need for healthcare professionals to narrow down an accurate antibiotic for the infection, and then its appropriate dosage to minimize acquiring bacterial resistance. Other drawbacks in managing MRSA related lung infections include low drug penetration of antibiotics in lungs administered via IV, which often end up in increased dose, poor diagnosis methods in detecting the susceptibility of *S. aureus* strain and close community living (**Figure 1.2**). With the development of resistance of MRSA towards Vancomycin and the limitations which arise from increasing the dose of Vancomycin in patients susceptible to toxicities, alternate treatment strategies are needed.

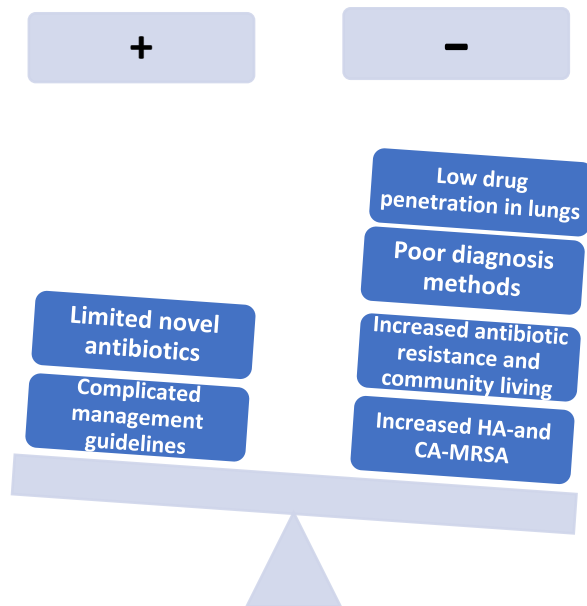


Figure 1.2 Current Scenario for Management of Antimicrobial Resistance

1.3 Nanomedicine Interventions in the Treatment of Lung Infections

Recently, nanotechnology has gained prominence in the development of efficient drug delivery systems with several advantages including increased bioavailability, improved patient compliance, reduced side effects, and targeting ability [29, 30]. Drug pharmacokinetics and pharmacodynamics depend on the formulation and delivery strategies of the drug carrier. Nanoparticles can provide advantages of controlling drug release, protecting biotherapeutic agents from degradation via enzymes, improving drug solubility, enhancing cell uptake of drug payload, and facilitating targeting ability towards infected cells. Inhalation delivery of nanotherapeutics has improved both local and systemic activity by exploiting the airway used by pathogens to cause lung diseases. The inhalation route of administration can bypass the first-pass metabolism leading to increased bioavailability of drugs in lungs. The nanotherapeutics (nanoparticles loaded with drugs) will be deposited or exhaled from the lungs based on the diameter of the nanoparticles. Particles with a

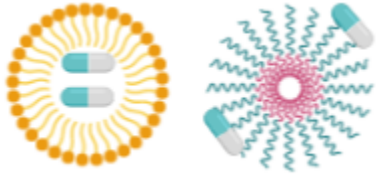


size ranging from 1-1000 nm have shown to get deposited deeper into the lower airway regions such as alveoli [31-33].

The major factors contributing to the popularity of nanotherapeutics are: **1) increased bioavailability, 2) enhanced drug targeting, 3) improved drug solubility and stability, 4) controlled drug release, and 5) facilitated patient adherence.** These properties of nanotechnology make it beneficial to effectively treat various lung diseases [34]. In a study done by Jurek et al. [35], edema in acute lung injury was prevented after 3 days via inhalation delivery of ruthenium red loaded PLGA nanoparticles over free ruthenium red in high-pressure mechanical ventilation (HPMV)-mediated mice ex-vivo perfusion studies, showing the potential significance of nanoparticle mediated drug delivery for treating patients with respiratory failures [35]. Similarly, free anti-inflammatory drug delivered to treat lung injury related inflammation in mice was almost undetectable in the lungs after 4 hours compared to targeted nanoparticles, which were seen for over 24 hours, in a study by Zhang et al. [36]. In another study, pretreatment with anti-inflammatory molecule α -bisabolol loaded lipid-core nanocapsule (LNC) in LPS-induced lung injury showed a higher concentration of the anti-inflammatory molecule in the lungs compared to free α -bisabolol [37]. Also, this study showed significant reduction in lung injury via LNC loaded α -bisabolol than free α -bisabolol. Various nanoparticles-mediated drug delivery approaches have been successfully utilized previously to treat acute lung diseases [38]. *The strategy of inhalable nanotherapeutics has proven to reduce the drug dosage level and the adverse complex drug interactions.* Use of nanoparticles to deliver antimicrobial drugs (both intracellularly and *in situ*) and other biologics to reduce lung injury via inhalation can improve drug bioavailability and enable targeting of the lower respiratory tract and pathogen infected lung epithelial cells to inhibit intracellular pathogens and reduce lung injury.

1.3.1 Type of NPs

Several types of biomaterials are available for the design of nanoparticles intended for pulmonary drug delivery. Polymer-drug conjugates are widely employed for pulmonary delivery where engineering of the biodegradable polymers provided protection of encapsulated drugs and improved overall stability of the formulations. Lipid-based carriers such as liposomes and micelles have also been employed for pulmonary delivery of drugs. Major types of nanoparticles used in pulmonary delivery are detailed as follows (**Table 1.1**).

Table 1.1 Types of Nanoparticles for Pulmonary Drug Delivery

 <p>Micelles (left: Lipid; right: Polymeric)</p>	 <p>Liposomes</p>	 <p>Polymer Nanoparticles</p>
<ul style="list-style-type: none"> - Single-layered phospholipid with hydrophobic core. - Biocompatible and can cross air-blood barrier when delivered via inhalation [39]. -Polymeric micelles are highly functionalized [40]. 	<ul style="list-style-type: none"> - Consists of phosphor lipid bi-layer with higher biocompatibility. - Hydrophilic core. Ability to encapsulate payloads of variable solubilities. 	<ul style="list-style-type: none"> - Consists of synthetic/natural polymer with ability to load both hydrophilic and hydrophobic payloads. - Substantial number of biomaterials available to synthesize polymeric nanoparticles.

1.3.1.1 *Micelles*

Amphiphilic molecules under certain conditions form micelles. Micelles can be formed from both lipids and polymers. Various poor water soluble drugs including paclitaxel, beclomethasone dipropionate, and budesonide are shown to be encapsulated by micelles formed from DSPE-PEG₅₀₀₀ [41]. Incorporation of PEG molecules can also improve the retention of micelles as shown by Gill et al. [42]. In this study, paclitaxel-based DSPE-PEG₃₀₀₀ showed higher AUC when compared to Taxol®, showing the micelle benefits for pulmonary delivery. Although micelle retention was high, their stability and delivery efficiency need to be assessed in lung infections, where bacteria are hard to access due to formation of biofilms and intracellular residence in phagocytes and epithelial cells. Polymeric micelles are more robust compared to lipids due to the larger repertoire of polymers available for the design of nanocarriers. Overall, even though micelles provide a pulmonary drug delivery platform, the exposure of drugs in micelles open architecture is prone to enzyme degradation, commonly seen in microenvironments of lung infections.

1.3.1.2 *Liposomes*

Liposomes consists of bi-layered phospho-lipid membranes with an aqueous core to entrap hydrophilic agents and hydrophobic agents as payloads between the bi-layer. Lung surfactants are majorly composed of lipids such as DPPC and SP-A-D among others. This makes liposomes favorable for pulmonary delivery. Arikace®, an anti-pseudomonal liposome formulation has successfully entered phase II clinical trials where drugs encapsulated in liposomes are delivered via inhalation to treat cystic fibrosis [43]. Similarly, liposomes are being employed to deliver steroids such as beclomethasone successfully via inhalation to treat asthma [43]. Some major factors, which pose a challenge to liposomes mediated delivery of antibiotics to lung infections, are the formulation stability, nebulization mechanism, targetability of infected cells with

pathogens, and intracellular residence and penetration of bacterial biofilms. There is a need for alternate drug delivery systems to address these concerns present in the use of liposomes for bacterial lung infections.

1.3.1.3 *Polymer nanoparticles*

Out of various nano formulations, polymeric nanoparticles have been extensively studied in pulmonary drug delivery. A large set of biomaterials, including natural polymers such as chitosan, alginate, gelatin, and cellulose, and synthetic polymers like poly(lactic-co-glycolic acid) (PLGA), poly ϵ -caprolactone (PCL), poly lactic acid (PLA), polystyrene, and poly ethylene glycol (PEG) are used for designing drug carriers for pulmonary drug delivery [28, 44]. Polyaldehyde dextran and dialdehyde carbomethylcellulose nanosuspensions made from spray drying resulting in 0.5-5 μm size appropriate for delivery via inhalation, were investigated and methodology reported by Jablczyńska et al. [45]. Both synthetic and natural polymer loaded with fluorescent protein encoded plasmids were successfully delivered via inhalation in Sprague Dawley rats showing the potential of polymeric nanoparticles to deliver payloads into lower tract lung regions [44]. Additionally, Menon et al. [44] reported successful delivery of therapeutic EPO proteins with sustained release more uniformly seen in synthetic polymeric PLGA nanoparticles compared to natural polymers. As seen from the recent reports, PLGA has been extensively used for pulmonary delivery of various encapsulated molecules including the Hepatitis B vaccine, rifampicin, pirfenidone, voriconazole, and siRNA, among others [28].

PLGA nanoparticles among other polymer NPs are ideal, due to the wide characterization studies available and their ability to load a broad range of antibiotics. For instance, PLGA nanoparticles delivering antibiotics against tuberculosis maintained therapeutic drug concentrations in the lungs for 9-11 days, reducing the total drug dose required systemically [46].

Surface modifications of the antibiotic loaded PLGA nanoparticles are highly sought after to improve uptake in targeted cells such as macrophages and lung epithelial cells to eradicate intracellular resident bacteria such as MRSA [47]. Unlike liposomes and micelles, the polymer consists of a matrix with a cross linked polymer, which slowly degrades in the humid environment and releases the drug encapsulated drug in a controlled fashion [28]. PLGA polymer with its capability to deliver payloads to deep alveolar spaces is a promising candidate for delivering antibacterial drugs via inhalation to the lower respiratory tract infections.

1.3.2 Peptide Coated Nanoparticles

With improvement of molecular technologies, synthesis of peptides and screening of peptide libraries has become easy, enabling isolation of potent bioactive molecules against target cells. Although several potent peptides are synthesized normally, they face many challenges for drug delivery applications which include lower binding affinities, enzyme degradation and short circulating half-lives [48]. Hence, there is a need to design or combine the peptides with other forms of carriers to utilize the functionality of peptides in a combinatorial approach. Nanoparticle peptide composites (NPCs) are an emerging array of nano-formulations, which can bring together functionalities of peptides and nanoparticles to enhance drug delivery. NPCs bring the advantages of coating targeted peptides on top of nanoparticles loaded with various drugs, improving cell specific drug delivery. Nanoparticles provide surface functionalization that can be utilized to conjugate different peptides for targeting. Similarly, cell penetrating peptides produced can be conjugated with different nanoparticles to improve cellular uptake of nanoparticles, increasing the drug or gene delivery to targeted cells, which are in a diseased state. Overall, NPCs are a new model of drug delivery vehicles, which give a wider range of functionalization for improving targeting and payload accumulation in tissues or cells. Especially in infected cells where bacteria

are residing intracellularly, cell membrane penetrating peptides can improve nanoparticle delivery loaded with antibiotics for cytoplasmic release and inhibition of intracellularly resident bacteria.

1.3.3 Cellular Uptake Mechanisms of NPs in Infected Cells

Antibiotics have been widely used against bacterial infections. Despite the success, there is an increased antibiotic resistance due to reduced bioavailability of antibiotics at the site of infection and a systemic overdose. Nanoparticles have shown promise in targeted delivery of antibiotics/drugs to improve drug bioavailability to the infected cells or infected site [28]. A major challenge in persistent lung infections is to eradicate the bacteria which survive intracellularly creating areas which are undruggable [49]. The cell uptake mechanism plays a significant role in the fate of nanoparticles delivered to the cells. Nanoparticle uptake is facilitated by various mechanisms as mentioned in **Table 1.2** [50].

Table 1.2 Different Endocytosis Mechanisms of Nanoparticle Cellular Uptake

Clathrin-dependent	Fast endophilin-mediated endocytosis (FEME)	Caveolin dependent pathway	Clathrin-independent	Macropinocytosis	Phagocytosis
Dynamamin dependent			Dynamamin independent		
Clathrin mediated endocytosis is facilitated by	FEME is mediated by endophilin A2 protein	Mediated by caveolin and cavin proteins.	Independent of receptor-ligand interaction and is	Alternatively named cell drinking. Cell uptake of large	Phagocytosis is driven by actin polymerization with

adaptor complex AP2, which recruits clathrin proteins and forms a clathrin-coated pit.	recruitment and actin polymerization when ligand-receptor interaction takes place.		a constitutive process.	volumes of fluid using this mechanism controlled by actin dynamics.	macropinosome structures fissioned with the influence of C-terminal binding protein 1 (CTBP1).
~100 nm	~60-80 nm	~100 nm	~60 nm	>200 nm	>200 nm

Nanoparticle cellular uptake depends on various factors including polarity or charge of the surface, size, passive or active transport as seen in receptor targeted nanoparticles, shape of nanoparticles, hydrophobicity, elasticity and surface modifications [51]. Endosomal escape strategies are widely employed in carrier design to improve the release of the drug into the cytoplasm to inhibit resident intracellular bacteria. Phagocytosis of bacteria of 1 or 2 μm is readily taken up, but the particles larger than 200 nm have shown to be taken up less compared to smaller particles showing a discrepancy in the ability of cells to uptake particles [51]. Similar uptake behaviors are seen in non-phagocytic cells, where uptake increases with particle size until 50 nm and then uptake reduces when the size of the nanoparticle increases. *This shows the need to control the surface properties of nanoparticles to facilitate higher uptake in infected cells.* The effects of bacterial infection on nanoparticle cellular uptake have not been studied in detail. Hence, more studies are needed to understand the rate of nanoparticle uptake in healthy and bacterial infected cells. Some viral infected cells show contrast patterns with few strains showing reduced uptake of nanoparticles, which gives signals towards alteration in uptake mechanisms of cells under infection in general [52].

1.4 Design Considerations of Drug Delivery Systems Targeting Bacterial Lung Infections

Various nanoparticles including liposomes, micelles and polymeric nanoparticles are widely employed to encapsulate antimicrobial drugs to enhance therapeutic effects. Pulmonary drug delivery is well established in treating diseases such as asthma, cystic fibrosis (CF), and COPD. Only one treatment involving tobramycin inhalation delivery to *P. aeruginosa* infection in CF patients is available, showing the need for better design and development of new treatments for lung infections. Inhaled nano-formulation success depends on various design aspects including targeted drug delivery to the lower respiratory tract, shortened treatment course, reduced side effects, nanoparticle size, and clearance [53]. Particles $<1\ \mu\text{m}$ are deposited and uptaken in the alveoli, whereas particles $>1\text{-}5\ \mu\text{m}$ are largely phagocytosed and particles $>5\ \mu\text{m}$ are exhaled [54]. Challenges for inhalation-based nanoparticle drug delivery includes (1) mechanical barriers such as impaction of inhaled nanoparticles in the mouth and nose, loss in large airway tract, narrowing of airway due to mucus hypersecretion and mucocilliary clearance; (2) chemical barriers such as enzymatic degradation; (3) immunological barriers such as phagocytosis by alveolar macrophages and (4) patient compliance with respect to inhalation technique [53]. Design of nanoparticles for inhalation-based drug delivery should consider lung pathophysiology to address these design considerations and challenges to the targeted/diseased site.

Bacterial lung infections pose additional challenges as the conditions of lung physiology are changed with ongoing immune responses and bacterial activity. A lung infection is accompanied by mucosal swelling, which narrows the airways and requires adjusting of the inhalation technique to accommodate narrow airways. Excess mucous deposition can affect the permeation of delivered nanoparticles to the injured epithelium, requiring a mucus permeating nanocarrier design. Lungs are designed to remove foreign particles by coughing or creating a

bronchospasm, which can reduce patient compliance and subsequently, therapeutic outcomes. Hence, nanoparticles of a desired size of $<1\ \mu\text{m}$ need to be considered to target lower respiratory tract cells such as alveolar epithelial cells. Bacterial biofilms formed in infected lungs are another challenge for delivering drug nanoparticles to the lower tract of infected lungs. Biofilms formed from bacterial colonies underneath the mucus layers can trap the antimicrobials released from nanoparticles. Also, various degradation enzymes in mucus can neutralize the antimicrobials leading to poor therapeutic outcomes. Smaller size nanoparticles can penetrate the mucus to deliver antimicrobials. Mucus penetration strategies such as inclusion of PEG, mucins, and nanofiber peptides coated on top of nanoparticles can help overcome the challenges of mucus and treat biofilms in lung infections [28].

1.5 Overview of Dissertation Project

Respiratory diseases occurring from lung infections account for more than 4 million fatalities every year around the world [55]. This research proposes the development of novel nanocomposites based on a combination of cell membrane penetrating nanofibers and biodegradable nanoparticles loaded with antibiotics to treat MRSA lung infections. The specific aims and innovation pertaining to the project are explained below.

1.5.1 Objectives

The long-term goal of this project is to develop biocompatible nanocomposites for the treatment of lung infections. Inhalable delivery of nanoparticles has gained attention recently. However, inhalable nanoparticle or nanocomposites targeting lung infections are limited, especially as no studies have been done to treat MRSA using this technique. The polymeric nanoparticles chosen to deliver antimicrobials can be modified to accommodate drugs targeting various other lung diseases. In addition, the combination of cell membrane penetrating nanofibers

and antimicrobial drug loaded polymeric nanoparticles can enhance nanoparticle uptake in infected cells. Therefore, the final objective of this research is to evaluate novel nanocomposites for their enhanced pulmonary drug delivery and treatment of MRSA lung infections.

1.5.2 Specific Aims

Aim 1: Synthesis and characterization of novel nanocomposites for enhanced pulmonary drug delivery. Nanofiber coated PLGA nanoparticles (Nanocomposites) will be synthesized and characterized for their physical properties including size, stability, uptake abilities and mucus permeation. Nanocomposites will also be evaluated for their cytocompatibility in healthy lung epithelial cells. Effects of freeze drying, and nebulization will be determined to assess translative potential of the nanocomposites. Lastly, the cell uptake ability of nanocomposites with respect to commercial cell penetrating peptides will be performed.

Aim 2: Antimicrobial nanocomposites for the treatment of antibiotic resistant MRSA lung infections. Antimicrobial drug loading into nanocomposites (AMNCs) will be performed and characterized for drug loading kinetics, cytocompatibility, and antimicrobial properties will be investigated in MRSA bacterial cultures with respect to their minimum inhibitory concentrations and zone of inhibitions. AMNC uptake kinetics in healthy and MRSA infected cells will be determined. AMNC potential of intracellular MRSA killing will be performed by delivery in media and via nebulization. *In vivo* biodistribution of AMNCs and plain nanoparticles will be performed to determine their distributions in mice lungs via inhalation.

1.5.3 Innovative Aspects

Firstly, this work of combining nanofibers made of peptides and nanoparticles for treating lung infections has not been reported in the literature. The results from this study would provide information for other researchers involving preparation of nanocomposites of a similar nature. Cell

uptake studies clearly show the potential of combining nanofibers with nanoparticles to enhance drug delivery in infected cells. Comparison studies of nanoparticle uptake in healthy and bacteria infected cells have not been done before, and results from our studies provide latest information on the behavior of lung cell uptake of nanoparticles in infected conditions. This novel combination of nanofibers and nanoparticles can open possibilities to deliver drugs or genes or other small molecule therapeutics to several other lung diseases.

1.5.4 Successful Outcomes

The successful outcome of this research will be helpful in the design and development of nanocomposite formulations combining nanofibers and nanoparticles. Bacterial infection has shown to cause stress on cells leading to reduced nanoparticle uptake. This research has developed a robust drug delivery platform which can improve nanoparticle uptake in infected cells leading to efficient therapies. Different nanofibers including fluorescent-labeled, pH-sensitive, and enzyme-sensitive nanofibers in combination with nanoparticles can enable imaging and stimuli-responsive drug delivery. Given the enhanced uptake of nanocomposites, gene delivery can be improved by employing nanofibers with site specific targeting abilities.

Chapter 2

SYNTHESIS AND CHARACTERIZATION OF NOVEL NANOCOMPOSITES FOR ENHANCED PULMONARY DRUG DELIVERY

2.1 Introduction

Nanotechnology has come of age and ultra-small sized (1-1000 nm) nanoparticles with high-surface-area-to-volume ratio are being employed to deliver drugs and other therapeutics. Drug encapsulating nanoparticles have been reported to increase drug bioavailability and drug release in targeted tissues [56]. This, in particular, is highly beneficial to reduce the dosing frequency, improving patient compliance [57]. Types of nanoparticles include polymer-based, dendrimers, liposomes, metal-based, and inorganic particles like silica, among others. Although nanoparticles are uptaken by different endocytosis mechanisms of cells, there is often an issue of targeting and the number of nanoparticles needed to exert a therapeutic effect [50, 58]. Emerging challenges for intracellular delivery include evading removal of NPs from circulation due to mononuclear phagocyte system, avoiding off-site targeting and pre-mature drug release, and efficiently delivering drugs/genes intracellularly need to be addressed to improve payload delivery at target cells/tissues [59]. Engineering strategies improving uptake of nanoparticles can have a profound effect in drug delivery towards diseased cells which are infected, undergoing senescence and other abnormalities having reduced uptake ability.

Peptides have gained interest in the field of bioengineering to provide cell membrane penetration and intracellular delivery, antimicrobial properties, and pH-sensitive linkage [48, 60]. A peptide library screening has enabled synthesis of effective binding peptides against various targets favoring the design of targeted drug delivery systems. Peptide development has its own challenges in the scenario of drug delivery varying from binding affinity to a targeted site to

maintenance of appropriate functional folding, enzyme degradation *in vivo* and short circulating half-life [48].

Nanoparticle peptide composites (NPCs) are promising candidates with potential to overcome limitations of nanoparticles and peptides and enjoy the advantages of both components in a drug carrier design. NPCs have been reported to show higher binding affinities and selectivity in comparison to single peptides and proteins [48]. With a vast range of nanoparticles and peptides synthesized, there is a high scope for engineering of nanocomposites to improve peptide functionality and nanoparticle properties. A recent study by Shoshan et al. [61] have reported peptide-stabilized platinum nanoparticles, which increased the solubility and showed selective toxicity towards liver cancer cells. Similarly, Ma et al. [62] coated platinum nanoparticles with mitochondria specific peptides, which improved the stability of platinum nanoparticles and helped accumulate these particles intracellularly, enabling the photothermal therapy using NIR light. These studies show the ability of peptide nanoparticle composites in targeted therapies. Other advantages of peptide-nanoparticle nanocomposites include targeted drug delivery based on specific peptide coating, enhanced drug delivery to improve cellular uptake, molecular imaging, and liquid biopsy in capturing extracellular vesicles such as exosomes [48]. Herein, we develop a novel nanocomposite combining cell penetrating nanofibers and biodegradable nanoparticles to enhance pulmonary drug delivery.

2.2 Methods

2.2.1 Materials Used

All chemicals, if not specified, were purchased from Sigma-Aldrich (St. Louis, MO). PLGA (copolymer ratio 50:50, Molecular weight 15kDa- 25kDa) was purchased from Akina Inc.

(West Lafayette, IN); Rhodamine B dye was purchased from Sigma-Aldrich (St. Louis, MO) and the nanofibers were synthesized in-house as previously described [63]. Primary human alveolar type 1 cells were obtained from Applied Biological Materials (Richmond, BC, Canada). Iscove's Modified Dulbecco's Medium (IMDM), Fetal bovine serum, penicillin-streptomycin, and trypsin-ethylenediaminetetraacetic acid (EDTA) were procured from Fischer Scientific (Waltham, MA). Amiloride, filipin III, and methyl- β -cyclodextrin were purchased from Sigma-Aldrich (St. Louis, MO).

2.2.2 Synthesis of Nanocomposites

A double emulsion method as described by Messerschmidt et al. [64] was employed for the synthesis of PLGA NPs. First, 100 mg of PLGA polymer was dissolved in dichloromethane at 100 mg/mL. 1%(w/w) Rhodamine B (Rho B) was prepared as a water phase, which was later added dropwise into the oil-phase of PLGA solution. This primary solution was sonicated to form the primary emulsion. The primary emulsion was emulsified into 5%(w/v) poly(vinyl) alcohol (PVA, 13KDa) solution via sonication at 35 watts for 4 minutes (30 seconds off every 1 minute). Rho B loaded PLGA nanoparticles were collected by centrifugation at 15,000 RPM for 15 minutes, then lyophilized until completely dry.

Nanofibers were synthesized as previously described by Su et al. [63]. Briefly, a standard Fmoc-solid phase peptide synthesis method on a Prelude® peptide synthesizer was employed. Crude peptide collected was dried under a vacuum overnight for HPLC purification [63]. Peptides purified were rehydrated with TRIS buffer for a period of 12 hours to self-assemble and form into nanofibers.

After lyophilization of nanoparticles, 2 mg of Rho B-NPs were dissolved in tris(hydroxymethyl)aminomethane (TRIS) buffer and 0.5 mg of nanofiber in suspension was added to the nanoparticle suspension. The mixture was left to react electrostatically by rotating the solution for an hour at room temperature. Later, the sample was centrifuged at 15,000 RPM for 7 minutes to remove free nanofibers and collect the nanocomposites which contained nanofiber-coated Rho B-loaded nanoparticles.

Plain PLGA NPs used for FT-IR studies were synthesized by a single emulsion method where the PLGA polymer was dissolved in chloroform followed by drop wise addition into 5% (w/v) PVA. The mixture was emulsified via sonication at 35 watts for 4 minutes (30 seconds off every 1 minute). Later the PLGA NPs were collected via centrifugation and lyophilized until dry.

2.2.3 Characterization of Nanocomposites

2.2.3.1 DLS *measurements*

ZETAPALS90 dynamic light scattering (DLS) detector (Brookhaven Instrument, Holtsville, NY) was used to determine size, charge, and polydispersity of the nanocomposites. For DLS measurements, 50 μ L of 1 mg/mL nanocomposite suspension was mixed with 3 mL of DI water in a transparent cuvette and placed in the instrument to measure size while a DLS probe was used to measure the zeta potential of the nanocomposites.

2.2.3.2 *Fluorescent microscopy*

Fluorescein terminated peptides were synthesized as previously described by Yang et al. [63]. 5(6)-carboxyl fluorescein (FITC) tagged peptides were mixed with Rho B PLGA NPs. Green color tagged nanofibers were incubated with nanoparticles loaded with Rhodamine B (red color).

The nanocomposites formed were washed 3 times to remove any unbound nanofibers. Another set of nanoparticles were similarly washed and imaged without any nanofiber. A fluorescent microscope (ECHO, San Diego, CA) with FITC (for nanofiber) and Texas Red Channel (For Rho B NPs) was used to image the nanofiber coating on the nanoparticles.

2.2.3.3 FTIR of nanocomposites

Freeze-dried material including PLGA polymer, plain PLGA nanoparticles, and nanocomposites made from plain PLGA NPs, and nanofiber were analyzed using Fourier-Transform infrared spectroscopy (FTIR). Briefly, FTIR spectra of the varied materials were recorded in transmission mode using FT-IR Nicolet-6700 in the range of 400 to 4000 cm^{-1} .

2.2.3.4 Binding kinetics of nanofibers to nanoparticles

Thermophoresis technique was used to detect binding of nanofibers (ligand) to the nanoparticles. F_{norm} represents the change in thermophoresis, which is expressed as change in thermophoresis when non-fluorescent ligand titration is introduced to fluorescent nanoparticles [65]. Here, nanofiber titrations were made starting from 2mg/mL of nanofiber up to 10 dilutions with nanoparticle concentration kept at 2mg/mL for all the titrations. Small capillary tube was used to load ~4 μL of the various nanofiber-nanoparticle combinations and placed in the loading tray of Thermophoresis instrument Monolith NT.115. (NanoTemper Technologies, Inc., San Francisco, CA). To determine the position of the capillaries, a fluorescence scan is performed. Subsequently, thermophoresis measurements were performed to determine the binding kinetics of nanofibers to nanoparticles. F_{norm} was calculated by the machine along with various other parameters including binding constant.

2.2.4 Cytocompatibility of Nanocomposites

Here we used primary lung epithelial cells to assess the toxicity from nanocomposites. Nanocomposites were prepared as described in section 2.2.2, whereas 20,000 cells/well of primary alveolar type I epithelial cells (AT1) were seeded in 48-well plates. After the overnight culture, various groups of particles including plain/blank PLGA NPs, nanofibers only, and nanocomposites (nanofiber coated PLGA nanoparticles) were given to the cells in triplicates at various concentrations ranging from 0.0625-1 mg/mL. The nanofiber concentration was chosen equivalent to the peptide amount conjugated to the nanoparticles. After 72 hours, cells were washed 3 times with PBS, and MTS reagent was given to the cells to assess the cell viability following the company's instructions.

2.2.5 Cellular Uptake of Nanocomposites

The cellular uptake study was performed as described previously by Iyer et al. [66]. Nanocomposites made from Rhodamine B PLGA NPs, and nanofibers were used as fluorescently labeled nanocomposites for cell uptake studies. Cell uptake of nanocomposites was determined by measuring internalized fluorescent nanocomposites. Various cell lines representative of the lower respiratory tract including AT1, and RAW macrophages were used to assess the nanocomposite cell internalization ability compared with plain/blank nanoparticles. This is a critical study for many other experiments throughout the thesis as we compare our nanocomposites (NCs) with nanoparticles (NPs) in respect to uptake and subsequently drug delivery ability associated with improved uptake. AT1 cells (15,000 cells/well) and RAW cells (20,000/well) were seeded onto a 48-well plate and were grown overnight at 37°C. After overnight attachment, various nanoparticles and nanocomposites with different concentrations (0, 50, 100, and 250 µg/mL) were given to the cells in media for 90 minutes. After 90 minutes, AT1/RAW cells were washed 3 times with PBS and lysed using 2% Triton X-100. Fluorescence intensity of internalized NPs or NCs were

measured at a wavelength of λ_{ex} 546 nm and λ_{em} 585 nm (for the Rhodamine B fluorescence loaded into the NPs/NCs). Cell lysate was used to determine the protein content using bicinchonic acid assays (BCA) per the manufacturer's instructions (Pierce™ BCA Protein Assay, Thermo Scientific).

For visualizing the cellular uptake before the cell lysis, the cells were stained for nucleus with NucBlue (Thermoscientific) for 20 minutes. After staining, cells were imaged using a fluorescent microscope (ECHO, San Francisco, CA) in the DAPI channel for nucleus and the Texas Red channel for NPs or NCs.

Time-dependent uptake of nanocomposites in comparison with nanoparticles was performed in lung epithelial cells. Briefly, AT1 cells were seeded at confluency and allowed overnight to attach. The next day, cells were treated with 0.5 mg/mL of nanocomposites and nanoparticles for uptake. At timepoints of 30 minutes, 90 minutes and 4 hours, cells were washed 3 times with PBS and lysed with 2% Triton X-100. Cell lysate was read for fluorescent particles using a plate reader. Later, the total cell protein content was measured using a BCA assay.

AT1 cells were seeded at confluency onto a glass slide to perform confocal studies for nanocomposite uptake. After overnight attachment, nanocomposites or nanoparticles at a concentration of 0.5 mg/mL were incubated with the cells for uptake. Cells were washed with 3 times PBS after 4 hours of uptake, and the cell nucleus was stained with NucBlue. Cells on the glass slide were mounted with a cover slip to visualize the internalization of nanocomposites using a confocal microscope (Nikon).

2.2.6 Mucus Permeation Study

A mucus permeation study was performed to study the effects of the nanofiber coating on permeation of the nanoparticles to mimic the *in vivo* environment. NCs/NPs loaded with Rhodamine B dye were used for the study. A 12-well transwell plate with a pore size of 0.4 μm was used for the study. Mucus was simulated based on previous literature [67]. Porcine mucin protein was mixed with salts, DNA and DPPC to form simulated mucus. 100 μL of simulated mucus was placed on the transwell membrane and 500 μL of PBS was placed in the lower chamber. 25 μL of 10mg/mL of NCs/NPs were placed on top of the simulated mucus to allow for permeation from transwell to the lower chamber. PBS from the lower chamber was collected at various timepoints to measure the fluorescent NCs/NPs permeated through the mucus. Fresh PBS was replaced at different timepoints.

2.2.7 *In vitro* Nebulization

To assess the cell uptake ability of aerosolized NCs, we used a nebulizer to deliver the nanocomposites and nanoparticles. AT1 lung epithelial cells were seeded at 0.4 million cells/well in a 12-well plate and grown overnight. 1 mg/mL of both NCs and NPs in PBS were aerosolized using a lab module nebulizer from aeroneb[®] (Kent scientific, Torrington, CT). Aeroneb generated 2.5-4 μm droplets of particulate suspension. After nebulization of droplets, cells were incubated at 37⁰ C for 90 minutes. After incubation, cells were washed with PBS and stained for the nucleus with NucBlue (Thermofisher). Fluorescent images were taken of the cells for uptake of nanocomposites and nanoparticles using a fluorescent microscope (ECHO, San Francisco, CA) under DAPI (nucleus) and Texas Red (NCs/NPs). Later, the cells were lysed using 2% Triton X-100, and cell lysate was read using a spectrophotometer at a wavelength of λ_{ex} 546 nm and λ_{em} 585 nm. The cell protein amount measured by a protein assay was used to normalize the fluorescent

readings from cells. Percentage and weight number of NCs/NPs delivered to the cells were calculated based on the normalized fluorescence readings.

2.2.8 Nanocomposite Cellular Uptake Mechanism Study

To determine the NC/NP uptake mechanism used by cells, we performed an endocytosis-inhibition examination. Alveolar Type I cells were seeded at confluency in 48-well plates and attached overnight at 37°C in an incubator with 5% of CO₂. Rhodamine B loaded nanocomposites were prepared using a similar procedure done for other studies. After 24 hours of seeding, the AT1 cell culture medium was replaced by fresh 1% serum media containing 5 µM of Amiloride, 5 µM of methyl-β-cyclodextran, 5 µg/mL of Filipin III, 5 µM of Cytochalasin-D, 5µM of Imipramine, 80 µM Dynasore, or 5mM of Deoxy-glucose (Sigma Aldrich & Cayman Chemical). After 2 hours, fresh complete media with Rho B-labeled nanocomposites were added removing the endocytosis inhibitors at a concentration of 0.5 mg/mL. After 12 hours, cells were washed with PBS and nuclei stained with NucBlue (Thermofischer). Images were acquired using a fluorescent microscope and processed for NP uptake random areas from 10 images of each inhibitor group with ImageJ software.

In a similar fashion, to check if the nanocomposite undergoes an energy-dependent uptake, temperature block was studied in AT1 cells by preincubating cells at 4°C for 30 minutes, followed by treatment with fluorescent nanocomposites for 90 minutes at 4°C. Later, fluorescent images were acquired, and cell lysate analyzed for quantitated nanocomposite uptake.

2.2.9 Effects of Nanocomposite Freeze-Drying

A cell uptake study was performed to assess the ability of nanocomposites to retain an enhanced uptake ability after freeze drying. Nanoparticles along with nanocomposites loaded with

Rhodamine B dye were freeze-dried until dry. Later, NPs and NCs from before and after the freeze drying were prepared using TRIS buffer and later washed and mixed with complete media. AT1 cells in 48-well plates grown to confluency were given various groups of NCs and NPs from before and after freeze drying samples at a concentration of 0.5 mg/mL. Cell uptake study was performed similar to previous procedure (see section 2.2.5).

2.2.10 Nanofiber Coated NPs vs. HIV TAT Peptide Coated NPs

HIV TAT peptide is a common cell penetrating peptide. This study was aimed to compare nanofiber coating and HIV TAT peptide coating for their enhanced cell uptake ability. HIV TAT peptide coating of PLGA NPs was done similar to nanofiber coating (see section 2.2.2). Briefly, 0.5mg of either HIV TAT peptide/nanofiber was mixed with 2 mg of nanoparticles by rotation at room temperature for an hour. Later, the nanocomposites with the HIV TAT/nanofiber coating were collected and mixed with complete cell culture media at 0.5 mg/mL. AT1 cells grown overnight at confluency were given the nanocomposite groups and allowed to uptake for 90 minutes. A cell uptake study was performed similar to previous procedure (see section 2.2.5).

2.2.11 Time-Dependent Uptake of Nanocomposites

The capacity of nanocomposite uptake in comparison with nanoparticles was done by studying the uptake at various time points. Briefly, NCs and NPs at a concentration of 0.5 mg/mL were given to AT1 cells grown overnight at confluency in a 48-well plate. Different plates were used for different timepoints (30, 90, 240 minutes). A cell uptake study was performed similar to previous procedure (see section 2.2.5).

2.2.12 Statistical Analysis

GraphPad Prism 8 (GraphPad Software Inc., San Diego, USA) was used to perform statistical analysis. One-way ANOVA with Dunnett multiple comparisons and Tukey's multiple comparison tests were done for all the analyses. Triplicate samples were used for all the studies if not specified.

2.3 Results and Discussions

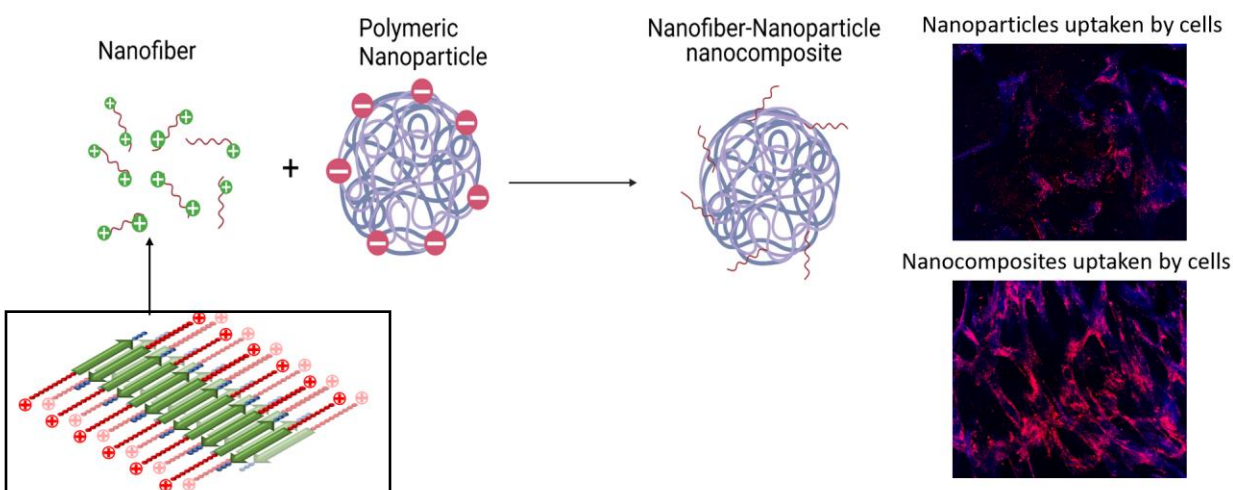


Figure 2.1 Schematic of Nanocomposite Synthesis. Black box represents the self-assembled peptides formed into a nanofiber.

2.3.1 Characterization of Nanocomposites

In this study, we prepared biodegradable PLGA nanoparticles, a commonly used nanoparticle, to develop our novel pulmonary drug delivery system [68]. PLGA nanoparticles have greater advantages as drug delivery vehicles due to high surface area, and polymer based nanocarriers have shown to deliver high concentrations of drugs with a prolonged release in lungs, avoiding systemic overdose from circulation of the intravenous delivery [69]. PLGA-nanoparticles prepared have a size of ~150 nm, which is suitable for lower respiratory tract delivery avoiding exhalation and upper respiratory tract accumulation [44]. Ohashi et al. [70] have formulated rifampicin-loaded PLGA nanoparticles of size ~213 nm and successfully delivered to alveolar

macrophages, while micron size particles were rapidly excreted from lungs [70]. For synthesis and *in vitro* testing of our nanocomposites made from nanoparticles and novel cell membrane penetrating nanofibers, we employed PLGA nanoparticles ranging from 150 – 200 nm. Novel self-assembled nanofibers prepared were mixed with PLGA nanoparticles loaded with Rhodamine B dye or plain PLGA nanoparticles to formulate nanocomposites at optimized concentrations. Both, dye loaded and plain PLGA nanoparticles were negatively charged as shown by zeta potential measurements (**Figure 2.2 A**).

Nanofibers presenting highly positively charge are coated on the surface of PLGA nanoparticles in the presence of TRIS buffer, as confirmed by the increase in size and reduction in surface charge of nanocomposites (**Figure 2.2 A**). Similar trends of reduction in the surface charge is observed in a recent study by Galindo et al. [71], where targeted peptides were conjugated onto PLGA nanoparticles for ocular delivery purposes. We also confirmed the presence of nanofibers on the PLGA nanoparticle by tagging the nanofiber with FITC. Our results show the presence of FITC labeled nanofibers co-localized with Rhodamine B labeled PLGA nanoparticles (**Figure 2.2 B**).

Furthermore, to confirm the nanofiber coated nanoparticles, nanoparticles were freeze-dried, and FTIR was performed to detect the presence of functional groups. An FTIR spectra of nanocomposites showed a distinct peak of amide I groups at 1640 cm^{-1} along with oop (C-H) bending from tryptophan rings seen at 750 cm^{-1} which is absent in PLGA nanoparticles without a coating (**Figure 2.2C**). PLGA was detected from the -CH aliphatic bond stretch at $2850\text{-}2950\text{ cm}^{-1}$ and -C=O carbonyl stretching (**Figure 2.2 C**). Thermophoresis technique was used to detect the binding ability of nanofibers onto PLGA nanoparticles. Here, Rhodamine B labeled NPs were used to detect thermophoretic kinetics in the presence of different concentrations of nanofibers. As

concentrations of nanofibers increased, the movement of dye labeled PLGA NPs reduced in the presence of infrared laser due to the binding of nanofibers onto PLGA nanoparticles, whereas at

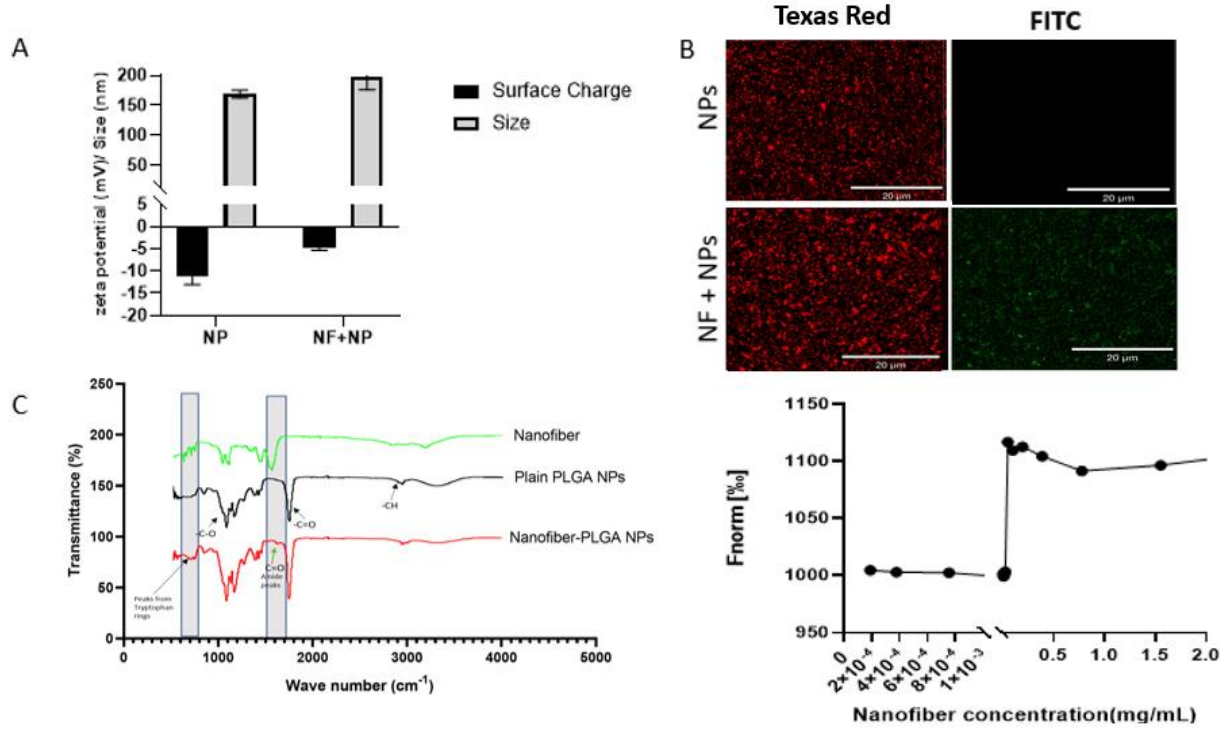


Figure 2.2 Characterization of Nanocomposites. **A.** DLS measurements of PLGA nanoparticles (NP) and nanocomposites comprising of nanofiber coated PLGA nanoparticles (NF+NP or nanocomposites) showing a slight increase in size along with reduction in charge due to a positively charged NF coating. **B.** FITC labeled nanofibers were coated with PLGA NPs loaded with Rhodamine dye. NPs alone do not have any fluorescence in the FITC channel (Green,) whereas fluorescence from FITC labeled nanofibers coated onto PLGA NPs can be seen in the bottom right channel. **C.** FTIR spectra of nanofiber coated PLGA NPs show amide I peaks at 1640 cm^{-1} from peptides of nanofibers along with peaks of oop (C-H) bending from tryptophan rings seen at 750 cm^{-1} . **D.** Binding kinetics using thermophoresis shows increasing the concentration of nanofibers reduced movement of Rhodamine B labeled NPs (fixed concentration) showing the effect of binding of nanofibers onto nanoparticles.

lower concentrations or only nanoparticles, faster movement of nanoparticles was shown (**Figure 2.2 D**). This shows the ability of nanofibers to bind to PLGA nanoparticles just by electrostatic interactions.

2.3.2 In Vitro Evaluation of Nanocomposites

Cell membrane penetrating peptides at higher concentrations have shown toxicity due to their membrane perturbations [72]. We investigated the cytocompatibility of nanocomposites

compared with nanofibers and nanoparticles individually. Plain nanoparticles and nanocomposites did not show any significant change of cytocompatibility up to 1 mg/mL in lung AT1 cells compared to the untreated control.

Lung epithelial cells were chosen as a model due to the disruption of the epithelial barrier by various virulence factors of MRSA such as Alpha-toxin (Hla), and Staphylococcal protein A (Spa)[73]. But nanofibers in equivalent concentrations present in nanocomposites showed significant reduction in cell viability in most of the concentrations (**Figure 2.3**). Nanofibers in combination with nanoparticles reduced their toxicity, which is seen when delivered individually. Cell membrane interaction of nanofibers coated onto nanoparticles needs further investigation, which can unravel the toxicities of using cell penetrating peptides or nanofibers alone. Overall, the cationic nature of nanofibers or peptides; for instance, can cause disruptive activity on cell membranes due to their affinity towards a negatively charged cell membrane [74]. From this result,

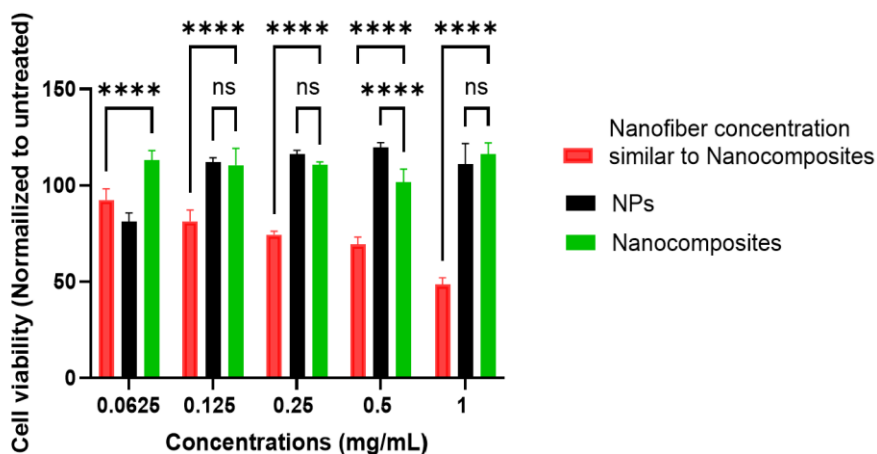


Figure 2.3 Cytocompatibility of Nanocomposites. Plain PLGA NPs with NF coating (Nanocomposites) and without Nanofibers (NPs) and nanofibers by themselves equivalent to conjugated in nanocomposites (Nanofibers) were given to Alveolar TYPE I cells seeded at 20,000 cells/well in a 48-well plate and grown overnight. After 72 hours of treatment with various groups, MTS assay was performed to assess cell viability. Nanofibers when conjugated to nanoparticles showed significantly less toxicity compared to when they are given directly. (**** $p < 0.0001$)

it suggests that combining cell membrane penetrating peptides or nanofibers with nanoparticle surfaces can reduce the disruptive activity and toxicity associated with them.

2.3.3 Enhanced Cell Uptake Ability of Nanocomposites

Novel nanofibers K₁₀Q₆E₃ have already been shown to possess cell penetrating abilities [63]. Their ability to improve nanoparticle uptake was studied in primary lung epithelial cells and RAW macrophages (**Figure 2.4**). These cells lines were used to assess the enhanced drug delivery abilities of nanocomposites for pulmonary drug delivery. Both AT1 and RAW macrophages

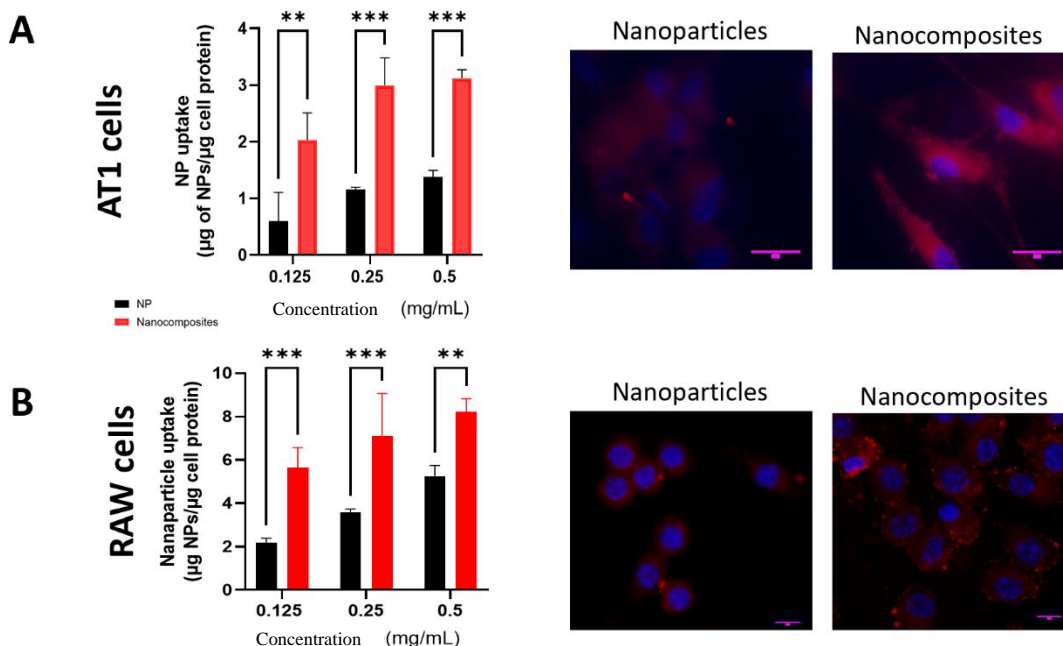


Figure 2.4 Cellular Uptake of Nanocomposites. A. PLGA nanoparticles with nanofiber coating (Nanocomposites) and without nanofibers (Nanoparticles) were given at various concentrations (0.125 – 0.5 mg) to overnight cultured primary lung AT1 epithelial cells in a 48-well plate (20,000 cells/well). (Scale 30µm) B. Similarly, nanoparticles and nanocomposites at various concentrations (0.125-05 mg/mL) were given to RAW macrophages (Scale 10µm). After 90 minutes, both cells were washed 3 times with PBS and stained with DAPI to take images with a fluorescent microscope. Later, cells were lysed with 2% Triton-X and a fluorescent reading for Rhodamine B dye was measured using a plate reader and compared with the dye standard while normalizing the fluorescent readings with cell protein content. Evidently, from both qualitative and quantitative data, nanofiber conjugation provides enhanced uptake compared to just nanoparticles. (* $P < 0.05$, ** $P < 0.01$, *** $p < 0.001$).

showed an increased uptake of nanocomposites (labeled with Rhodamine B dye) compared to nanoparticles (also labeled in Rhodamine B dye). RAW macrophages due to their intrinsic

phagocytic activity showed a higher uptake of nanocomposites compared to lung epithelial cells (**Figure 2.4**). This data shows that cell membrane penetrating nanofibers, when coated onto nanoparticles, can improve the nanoparticle delivery to cells and subsequently, the drugs carried by the nanoparticles, enhancing drug delivery.

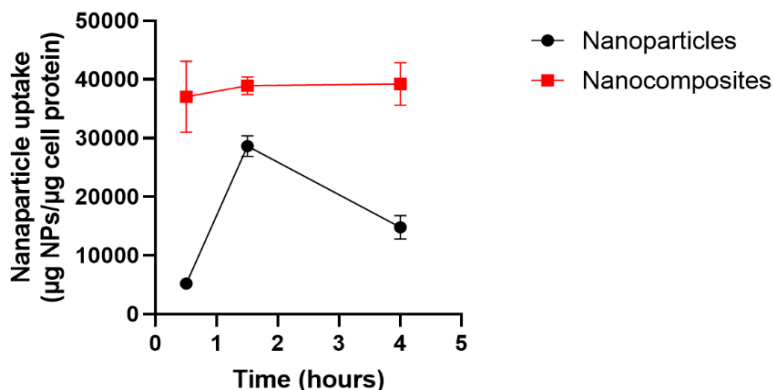


Figure 2.5 Time-Dependent Uptake of Nanocomposites. PLGA NPs with NF coating (Nanocomposites) and without Nanofibers (Nanoparticles) were given to Alveolar TYPE I cells seeded at 20,000 cells/well in a 48-well plate and grown overnight to form a monolayer. At various timepoints of 30 minutes, 90 minutes, and 4 hours, cells were washed and lysed to quantify fluorescent particles using a plate reader, and the cell protein from each well was used for normalization. Nanocomposites showed higher uptake and maintained the increased uptake compared to lower uptake of nanoparticles at each timepoint.

Uptake kinetics of nanocomposites were performed over 4 hours to understand the time-dependent uptake in lung epithelial cells. This study can help understand dosage time required and design therapeutic dosages needed to be delivered to the cells. Nanocomposites immediately attached to the cells in a few minutes, and later were internalized by the cells over a 24-hour period. Unlike nanocomposites, nanoparticles without nanofiber coating showed a linear increase in uptake until 90 minutes, and later plateaued with reduction in nanoparticles internalized (**Figure 2.5**). This reduction may be due to various phenomena such as exocytosis of NPs as extra cellular vehicles or other mechanisms [58].

Due to the positive charge of nanofibers and their affinity to the cell membrane, nanocomposite uptake was assessed to validate the internalization using a confocal microscope. Stacks of confocal cross-sections of AT1 cells acquired (**Figure 2.6**) show internalization of nanocomposites. Nanocomposites were localized in the x, z and y, z slices (marked with red boxes in **Figure 2.6 B**) along with DAPI stained nucleus membrane, which can be seen in the nanoparticle group, but at a lower quantity.

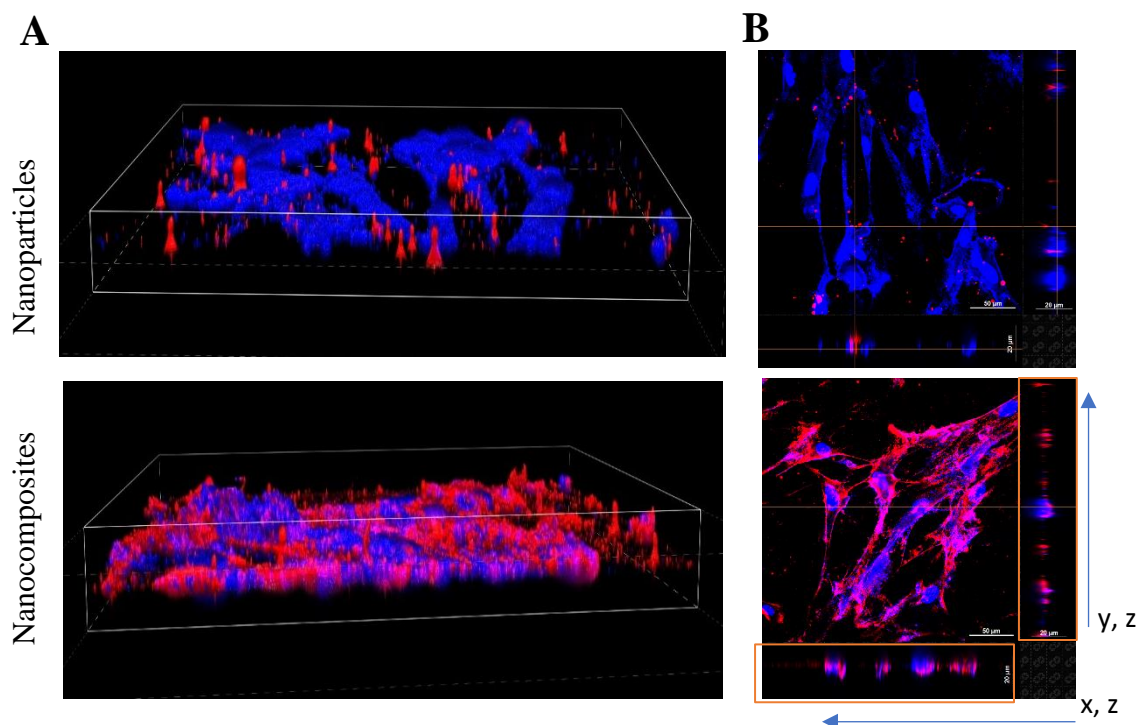


Figure 2.6 Confocal Imaging of Internalized Nanocomposites in AT1 Cells. **A.** 3D reconstruction of a confocal analysis of Alveolar epithelial cells exposed to nanoparticles (Top) and nanocomposites (bottom). **B.** 3D reconstruction of x, z and y, z-slices of the corresponding regions of image 2.5 A. showing the internalization of nanoparticles (Top) and nanocomposites (Bottom) with a higher amount seen in nanocomposites. Scale bar x, y - 50 μ m, x, z - 20 μ m, y, z - 20 μ m.

2.3.4 Permeation of Nanocomposites

Penetration of the mucus layer is highly desired to reach the injured epithelium in lungs due to the diseased state including infections and fibrotic conditions, among others. Especially in the case of lung infections, mucus hypersecretion is observed due to an increase to inflammatory signaling [75]. Hence, it is vital to understand the mucus permeation of nanocomposites. Adhesion

of nanoparticles to the mucus fiber is a challenge, and control of the size of the nanoparticle can improve the permeation. Recent reports suggest that nanoparticles <500 nm with a mucus inert coating can navigate through the mucus layer [76]. Here, we assessed the mucus permeation of nanoparticles with and without the nanofiber coating using a simulated mucus layer. Nanocomposites labeled with Rhodamine B were layered on top of simulated mucus, and its permeation through mucus and a 0.4 μm pore size transwell into the lower chamber was recorded to assess permeation kinetics. Nanocomposites traversed at a significantly higher rate compared to nanoparticles until 8 hours, and later, the permeation rate was similar to nanoparticle permeation kinetics (**Figure 2.7**). Overall, more nanocomposite particles permeated through the mucus than

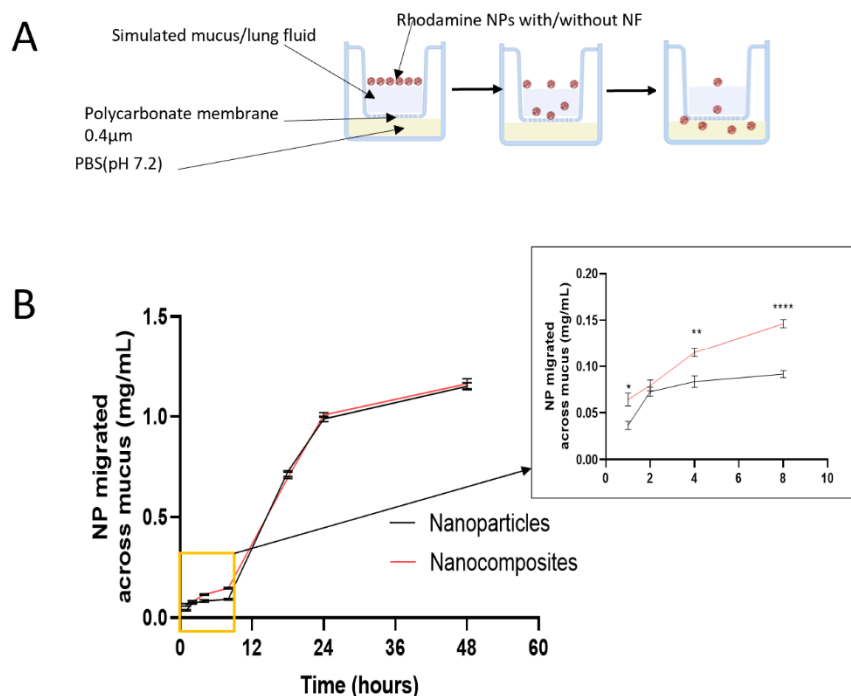


Figure 2.7 Mucus Permeation Study. *A. Schematic of mucus penetration setup. B. 50 μL Nanoparticles and Nanocomposites (nanoparticles with nanofiber coating) loaded with Rhodamine B dye at 10 mg/mL were laid on top of simulated mucus in a transwell plate with 0.4 μm pore size, with PBS in the lower layer. At various timepoints (0-48 hours) lower PBS solution was collected and measured using a plate reader. Nanocomposites have a greater penetration initially until 8 hours and later follow similar penetration kinetics as nanoparticles. (* $P < 0.05$, ** $P < 0.01$, *** $p < 0.0001$)*

through the nanoparticle alone, showing that nanofibers may interfere with nanoparticle binding to mucin proteins.

2.3.5 Uptake Mechanisms of Nanocomposites

A study of the uptake mechanism in nanocomposites can help understand the delivery efficiency and translation of results in other cell types [50]. Most nanoparticles are up taken by cells using endocytic or phagocytic pathways, including clathrin, caveolin, micropinocytosis, and other energy independent pathways. Previous studies have shown us that self-assembled nanofibers consisting of K₁₀Q₆E₃ peptides are uptaken by micropinocytosis when given to HeLa cells [63]. Nanofibers coated onto nanoparticles may not assume the same shape and orientation

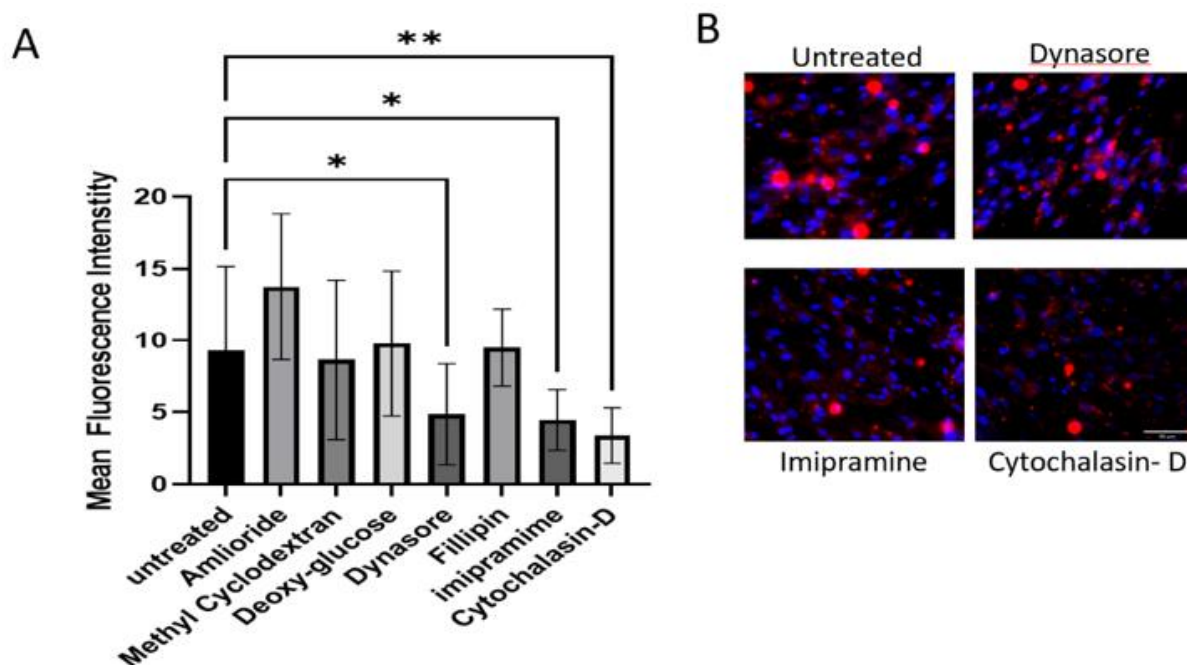


Figure 2.8 Cell Uptake Mechanism Study. **A.** Mean fluorescence intensity of uptaken nanocomposites after treating cells with various endocytosis inhibitors for 2 hours and allowing to uptake the nanocomposites for 90 minutes. **B.** NucBlue stained nucleus and Rhodamine B labeled nanocomposites show a representative image of nanocomposite uptake in AT1 cells (Scale 90 μ m). Multiple comparisons done using Benjamini, Krieger and yekutieli two-step linear step-up method. * $p < 0.05$, ** $p < 0.01$

and may not be freely available to resemble the activity seen in our previous studies. We screened the nanocomposite for their uptake mechanism using various endocytosis inhibitors. Lung epithelial cells after treatment with various endocytosis inhibitors and low temperature were treated with nanocomposites. Similar to the free nanofiber activity in HeLa cells, macropinocytosis inhibitors of cytochalasin-D and Imipramine showed significant reduction compared to untreated cells in uptake (**Figure 2.8**). This shows nanocomposites are up taken by macropinocytosis by the lung epithelial cells. Although, among the various macropinocytosis inhibitors, some of them did not show a significant difference to untreated cells, which shows the variation in inhibitor effects in various cell lines [50].

Similarly, lung epithelial cells were incubated at 4⁰C prior to the giving of nanocomposites to assess the energy dependency on uptake. Fascinatingly, NC cellular uptake was significantly higher than nanoparticles when cells were incubated at 4⁰C, showing the ability of nanocomposites to diffuse thorough the cell membrane independent of energy (**Figure 2.9**)

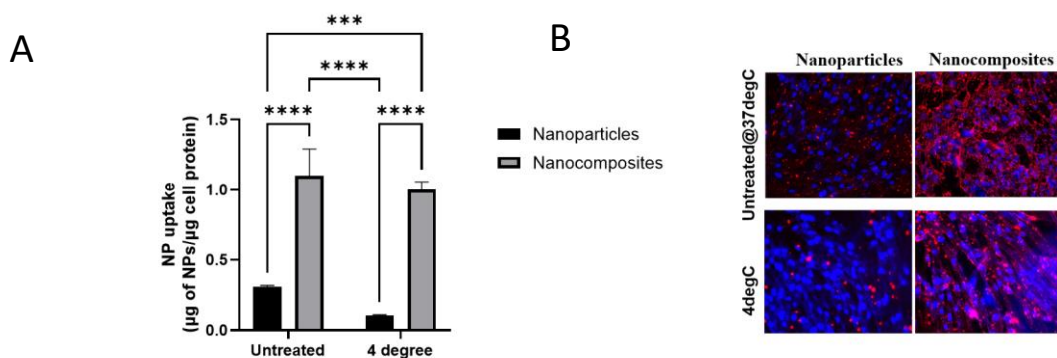


Figure 2.9 Cell Uptake of Nanocomposites at Low Temperatures. *A. Mean fluorescence intensity of up taken nanocomposites after incubating AT1 cells for 60 minutes at 4⁰C and allowing to uptake the nanocomposites for 90 minutes at 4⁰C. B. NucBlue stained nucleus and Rhodamine B labeled nanocomposites show a representative image of nanocomposite uptake in AT1 cells. Two-way ANOVA was performed with Tukey's multiple comparisons test. *** $p < 0.001$, **** $p < 0.0001$*

2.3.6 Translative Potential of Nanocomposites

Nanoparticle-based drug delivery systems are being developed at an explosive rate, but very few have reached the clinical trial stage [77]. This is due to the challenges associated with translation such as large-scale manufacturing, stability, delivery, and safety, among others. Here we assessed the stability in storage and nebulization for their potential in pulmonary drug delivery. Freeze drying of nanocomposites still showed significantly higher uptake in lung epithelial cells compared to nanoparticles (**Figure 2.10E**) demonstrating the storage ability of nanocomposites in powder form. Nanocomposites also showed higher uptake compared to a conventional cell membrane penetrating HIV TAT peptide coated nanoparticles (**Figure 2.10 F**). This indicates the superior ability of the nanofiber to improve nanoparticle affinity towards the cell membrane. Nanocomposites in powder have shown to possess higher stability compared to nanoparticles, suggesting the stability of the nanofiber binding of nanoparticles after undergoing freeze drying and storage at -20°C . Inhalation has recently gained attention as an ideal mode of pulmonary drug delivery [28, 53]. To assess the abilities of nanofibers to improve the nanoparticle uptake in cells when nebulized, nanocomposites and nanoparticles were delivered to lung AT1 cells *in vitro* via a lab module nebulizer generating droplets of size 2.5-4 μm (**Figure 2.10D**). Nanocomposites delivered via nebulization showed improved uptake with deposition efficiency over 23% delivered compared to 3% of nanoparticles (**Figure 2.10A-C**). Similar studies of *in vitro* nebulization showed fluorescein deposition efficiency of $<10\%$ [78]. Nebulization studies *in vitro* show that nanocomposites delivered via inhalation have the potential to enhance pulmonary drug delivery compared to PLGA-based nanoparticles.

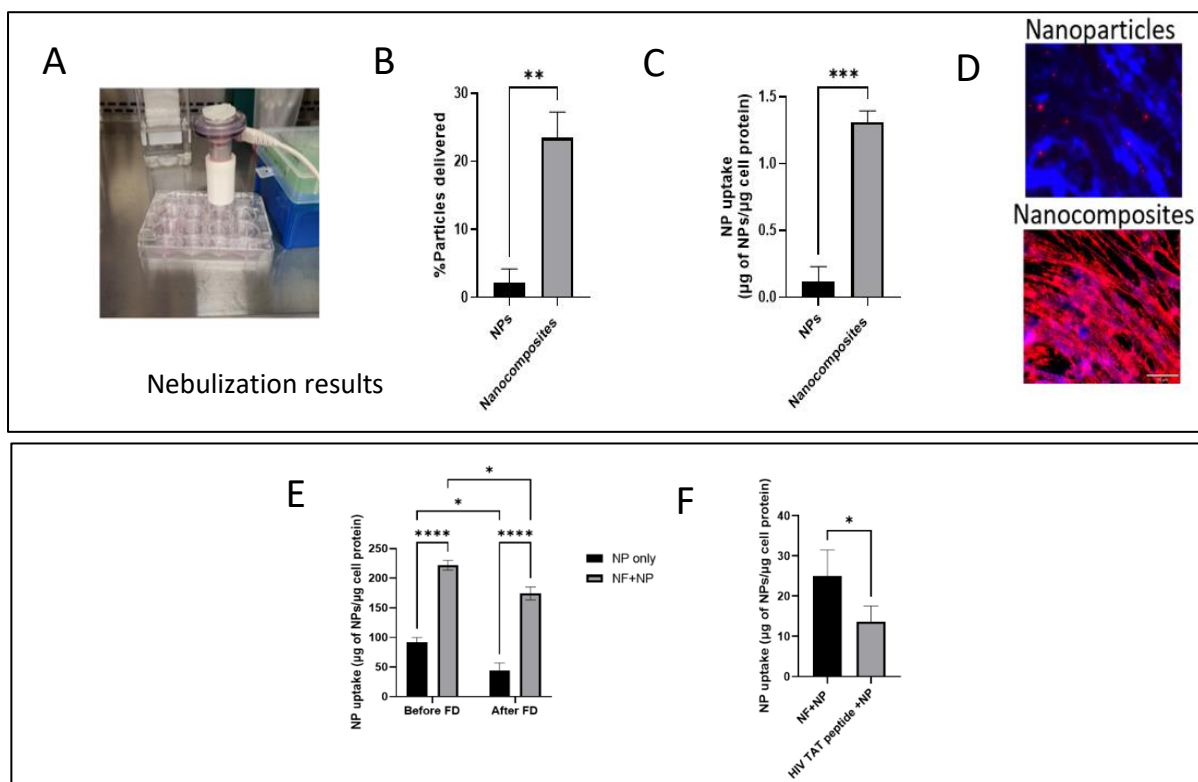


Figure 2.10 Translative Potential of Nanocomposites. AT1 Lung epithelial cells were seeded at confluency in a 12-well plate and grown overnight. 1 mg/mL of nanoparticles and nanocomposites (NF+NP) were nebulized using aeroneb® lab module nebulizer to generate droplets of size 2.5- 5 μm . After 90 minutes, cells were washed 3 times with PBS and stained with DAPI to visualize the uptake. Later, cells were lysed to analyze NP uptake by a fluorescent reading using a plate reader, and the measurements normalized against cell protein. **A.** Image showing nebulizer and 3D printed extension attached to deliver nanoparticles and nanocomposites to cells in a 12-well plate. **B.** % uptake after delivery of NPs and nanocomposites (NF+NP) via nebulization. Number of particles uptaken per amount of cell protein. **C.** Number of particles uptaken per amount of cell protein **D.** Fluorescent images after nebulization showing cell nuclei stained with DAPI and NPs loaded with Rhodamine B (Scale 90 μm). **E.** Before and after freeze drying effects on cellular uptake of both nanoparticles and nanocomposites. **F.** Comparison on effects of nanofiber and TAT peptide coating. Nanofiber coating shows significantly higher uptake of nanoparticles in AT1 cells compared to HIV TAT cell membrane penetrating peptide available commercially.

2.4 Conclusion

Our findings demonstrate that using nanofibers made from self-assembled peptide coating of polymer nanoparticles such as PLGA NPs can improve their uptake in lung epithelial cells *in vitro*. The nanofiber coatings effectively improve nanoparticle uptake in macrophages along with

epithelial cells. Both cell lines respond to bacterial pathogens and have high activity in lung diseases such as infections. In addition, the nanocomposites were delivered across in a faster simulated mucus layer, showing the ability to permeate the mucus layer more efficiently. With the evident potential for translation seen in freeze drying and nebulization studies, these nanocomposites can be extended to develop the next generation of pulmonary drug therapeutics involving advanced gene and drug delivery to treat a variety of lung diseases. Further modification of nanofibers can include targeted approaches with nanofiber peptides and nanoparticle conjugation strategies.

Chapter 3

ANTIMICROBIAL NANOCOMPOSITES FOR THE TREATMENT OF ANTIBIOTIC RESISTANT MRSA LUNG INFECTIONS

3.1 Introduction

Lung infections such as MRSA have been on the rise with increased antibiotic resistance and closed community living, leading to a need for the development of an efficient drug delivery system. For successful treatment, an efficient drug carrier is critical to deliver drugs, including antibiotics, to the site of infection. Current treatments of healthcare-associated and community-associated MRSA pneumonia intravenous administration of Vancomycin, Linezolid, or Clindamycin for a susceptible strain [79]. In some cases of antibiotic resistant bacteria, various antibiotic combinations are recommended. Use of IV antibiotic administration is a systemic approach with off-site targeting of drugs leading to adverse effects including nephrotoxicity, ototoxicity, and development of antibiotic resistance [27, 79]. Aging is a known risk factor for infectious diseases, especially closed community living more common in urban areas. Patient compliance to potent antibiotics is reduced in the aging population with weakened immune systems and low tolerance to adverse side effects from combinatorial therapies for antibiotic resistant bacteria. Hence, strategies to improve the efficacy and compliance of pulmonary drug delivery needs to be explored.

Inhalable formulations are mostly desired when designing drug delivery technologies to treat lung diseases due to the ability to deliver deep within the lungs overcoming the barriers of first pass metabolism, avoiding off-site targeting seen in IV administration, and reducing drug dosage based on targeted delivery [28]. Inhalable delivery can target lower tract lung infections

such as MRSA infections with aerosolized nanoparticles with improved properties to overcome barriers such as bacterial biofilms, a mucus layer and cell targeting to inhibit infectious pathogens. Various devices including nebulizers, metered dose inhalers, and dry powder inhalers are employed to deliver aerosolized drug carriers such as nanoparticles and/or microparticles.

Drug-loaded polymeric nanoparticles have been extensively studied for their benefits such as drug delivery systems to treat lower respiratory tract lung infections; especially polymeric nanoparticles with their properties including biodegradability, controlled drug release, and cellular uptake in a targeted approach via protection of drugs from enzyme degradation enroute [28, 44, 80, 81]. Out of the various polymeric nanocarriers, PLGA nanoparticles in specific have shown to deliver genes and drugs to the lower respiratory track via inhalation and even IV administration, facilitated with their easy synthesis, GRAS material designation and cost effectiveness [51, 82]. PLGA nanoparticles have also been used to load various antibiotics, including Rifampicin, Isoniazid, and Pyrazinamide as well as other drugs such as Pirfenidone for pulmonary delivery [83-86]. Due to several advantages and promise shown by PLGA NPs for pulmonary delivery, we selected PLGA NPs as our drug carrier to load antibiotics to treat MRSA infections.

Despite the advanced features of PLGA NPs to deliver to lower respiratory tracts, infection may change cell uptake behaviors. MRSA infection in lung epithelial cells of A549 has shown to reduce the nutrient uptake and enter a growth arrest [87]. Although there are not any studies which have investigated nanoparticle uptake in bacteria infected cells, some studies show mixed results of nanoparticle uptake in virally infected cells. For instance, Abo-Zeid et al. [52] studied negative surface charged polymer nanoparticles, which showed both a decrease and increase of NPs based on the variant of rhinovirus used to infect the HeLa cells [52]. Our preliminary results with various MOI of MRSA infection in lung cells have shown a reduction in NP uptake, which may be due to

cell growth arrest or poor nutrition of the cell [87]. Overall, to aid the nanoparticles for higher uptake in MRSA infected cells and delivery of antibiotics subsequently, nanocomposites consisting of surface coated novel cell membrane penetrating nanofibers are employed in our research. Herein, antimicrobial nanocomposites (AMNCs) loaded with Vancomycin were evaluated for their therapeutic efficacy *in vitro* and biodistribution in an *in vivo* setting.

3.2 Methods

3.2.1 Materials

All chemicals, if not specified, were procured from Sigma-Aldrich (St. Louis, MO). PLGA with 50:50 copolymer ratio and molecular weight of 15-25kDa was purchased from Akina Inc. (West Lafayette, IN). Vancomycin hydrochloride was purchased from Cayman Chemicals (Ann Arbor, MI). Methicillin-resistant *Staphylococcus aureus* (MRSA) USA300 strain was purchased from ATCC (Manassas, VA). Brain Heart Infusion (BHI) bacteria culture powder, Resazurin, was purchased from Sigma-Aldrich. Petri dishes, sterile discs for zone of inhibition study, and Agar were purchased from Fischer Scientific (Waltham, MA).

3.2.2 Synthesis of Antimicrobial Nanoparticles

A double emulsion method was used to produce Vancomycin loaded PLGA NPs. In brief, 100 mg of PLGA was dissolved in 4 mL of DCM, and 50 mg of Vancomycin hydrochloride was dissolved in 0.5 mL of Deionized (DI) water with 3 mg of dextran sulphate added to the solution. Vancomycin solution was emulsified with PLGA solution by sonicating at 40% power of the device with 2 cycles – 1 minute ON and 30 seconds OFF). Later, the primary emulsion was added dropwise into 5% (w/v) PVA under stirring. A second emulsion was creating by sonicating the

above solution using a Branson sonicator with 25 Amp with 4 cycles (1 minute ON and 30 seconds OFF). The second emulsion was left for stirring at room temperature to remove the DCM solvent. Nanoparticles formed were collected via washing and centrifugation and freeze dried until dry.

3.2.3 Synthesis of Antimicrobial Nanocomposites (AMNCs)

Antimicrobial nanoparticles of 2 mg loaded with Vancomycin were resuspended in TRIS buffer and mixed with 0.5 mg nanofiber for an hour at room temperature. Nanofiber was synthesized as previously described by Yang et al. [63]. Later, the nanocomposites formed by the coating of nanofiber onto nanoparticles were collected via centrifugation at 15,000 rpm for 7 minutes at 4°C. The nanocomposite pellet was then re-suspended in various buffers or media as needed for the experiments.

3.2.4 Characterization of Antimicrobial Nanoparticles

AMNCs were characterized for their morphology using TEM. Briefly, AMNCs were dropped onto copper grids and excess AMNC suspension was removed. Later, copper grids were treated with 0.1% uranyl acetate for negative staining of the AMNCs. Samples of AMNCs on the copper grid were imaged with a high-resolution TEM (Hitachi H-9500).

Vancomycin drug release profile from the AMNCs with and without the nanofiber coating was measured via dialysis and protein assays. Briefly, triplicates of 3 mg AMNCs and Van-PLGA NPs were dispersed in 1 mL of PBS (7.4) and dialyzed against a 3kD tubing with a sink reservoir volume of 10 ml. At every timepoint up to 48 hours, 1 mL of reservoir volume was collected and replaced with fresh PBS. After collecting samples, protein quantification assay (BCA) was used to assess Vancomycin release from collected samples by measuring using a Vancomycin standard.

AMNCs stability was evaluated by monitoring the size over a period. AMNCs suspended in saline were measured for their size over 3 days via Dynamic light scattering technique (DLS).

3.2.5 Cytocompatibility of AMNCs

To test the cytocompatibility of AMNCs, two different epithelial cell types residing in the lower respiratory tract were chosen (i.e., primary alveolar Type I epithelial cells (AT1) and Type II cells mimicking A549 cell lines). Both AT1 and A549 cells were seeded at confluency and allowed to attach overnight. The next day, various concentrations (0-1 mg/mL) of AMNCs were given to the cells by replacing the culture media with fresh media containing the particles. After 72 hours, cells were washed 3 times with PBS and given MTS reagent to assess the cell viability. Absorbance from cells after adding MTS was recorded using a plate reader (Tecan) and plotted in GraphPad prism by normalizing against untreated groups.

3.2.6 Cell Uptake of NCs in Infected Cells

Nanocomposite uptake ability in infected cells was measured via flow cytometry and quantifying internalized nanocomposites (vs. nanoparticles) using fluorescence techniques. Briefly, Alveolar Type 1 epithelial cells (AT1) were seeded at confluency in a 24-well plate. After overnight culture, the cells were treated with overnight grown MRSA bacteria in the various ratios (cell: bacteria; 1:0.5, 1:1, 1:10, 1:100). The co-culture of cells and bacteria were spun down at 2000 rpm for 5 minutes to settle bacteria and improve interaction of the bacteria and AT1 cells for infection purposes. After centrifugation, the cells were incubated with bacteria for 4 hours for infection and later washed 3 times with PBS (3xPBS) and treated with 100 µg/mL of gentamycin to remove extracellular bacteria. Nanoparticles and nanocomposites (nanoparticles with nanofiber coating) were added to the infected cells at 0.5 µg/mL and incubated for 90 minutes. After 90 minutes, cells were washed with 3x PBS and stained with NucBlue (Thermofischer) for visualizing

the nucleus. Images were taken for cell uptake using a fluorescent microscope (ECHO, CA). Later, cells were lysed with 2% Triton X-100, and cell lysate was used to quantify Rhodamine labeled nanoparticles and nanocomposites.

3.2.7 Antimicrobial Properties of Antibiotic Loaded Nanoparticles

Antimicrobial properties of nanoparticles loaded with Vancomycin were tested via minimum inhibitory concentration (MIC) and zone of inhibition assay's (ZOI).

3.2.7.1 *Minimum inhibitory concentration (MIC) assay*

A MRSA colony was picked and grown in BHI media overnight. The next day, MRSA was diluted to 1×10^6 CFU/mL for testing the MIC of Vancomycin loaded PLGA nanoparticles (Van-PLGA NPs). Briefly, Van-NPs were serially diluted in BHI media with various concentrations (1.5-1000 $\mu\text{g/mL}$) along with only BHI media and 1X MIC of free Vancomycin (positive control) and BHI media with MRSA only (negative control). 1×10^6 CFU/mL was mixed with various concentrations of Van-NPs in 1:1 ratio and incubated at 37°C for 24 hours. After 24 hours, 0.015% resazurin was given to the various test groups and incubated further for 1 hour. Later, pictures were taken to assess the color change in the test groups. Resazurin changes to pink indicating growth of bacteria, whereas it remains blue if no bacterial growth is observed.

3.2.7.2 *Zone of Inhibition*

Zone of Inhibition studies were performed to assess the antimicrobial potential of Van-PLGA NPs in comparison with free Vancomycin. Briefly, 200 μL of 1×10^8 CFU/mL of MRSA bacteria was plated onto BHI agar plates. 7 mm sterile discs were loaded (50 μL) with various groups of 1X, 2X MIC of free vancomycin and equivalent Van-PLGA NPs along with negative controls of plain PLGA NPs and BHI media. The loaded discs were placed on the MRSA plated

agar plates in triplicated fashion and incubated for 24 hours. Later, pictures were taken of each disk with scale to measure the diameter of the Zone of Inhibition of bacterial growth.

3.2.8 Intracellular Killing Efficiency of AMNCs

To assess the intracellular killing efficacy of AMNCs, an intracellular killing study was performed as described previously [88, 89]. Briefly, AT1 cells were seeded at confluency in a 24-well plate and allowed to attach overnight. The next day, 1:10 (cell: bacteria) ratio of MRSA was given to the cells via re-suspension in AT1 cell growth media, followed by centrifugation to facilitate bacterial infections in the exposed cells. After 3 hours, cells were washed with 1X PBS and incubated 30 minutes with gentamycin at a concentration of 100 µg/mL to remove the added bacteria. Cells were washed and various treatment groups of 0.5 mg/mL each of Van-PLGA, AMNCs, and free Vancomycin drug (concentration of free drug is equivalent to the drug loaded into nanoparticles) for 12 hours. After 12 hours, cells were washed three times with 1X PBS and lysed with either Di water or 0.02% Triton X-100. Serial diluted cell lysate was plated onto BHI agar plates to quantify the number of intracellular MRSA bacteria. Bacterial quantifications are represented as log 10 CFU per well.

3.2.9 Nebulization of AMNCs

In vitro nebulization was performed to assess the nebulized AMNC *in vitro* therapeutic efficacy [78, 90]. AT1 cells were seeded at confluency in a 12-well plate and allowed to attach overnight. The next day, AT1 cells were infected with bacteria (1:10, cell: MRSA bacteria) as mentioned in the previous section. Next, 1 mg each of Van-PLGA and AMNCs were loaded into a lab module nebulizer (aeroneb[®]) along with equivalent amounts of free Vancomycin dissolved in 1 ml of PBS. The above treatment groups were nebulized on top of the cells using a 24-well

trans well insert with the membrane removed. This was to facilitate airflow exit for the nebulized particles. After treatment with particles for 12 hours, cells were washed with PBS and lysed with DI water. Serially diluted cell lysate was plated onto a BHI agar plate and log 10 CFU was calculated from each well to determine the MRSA killing from different treatments.

3.2.10 *In Vivo* Biodistribution of Nanocomposites

To assess the lower respiratory tract targeting capability of nanocomposite formulations, we performed a biodistribution study in mice. For this study, 7–10-week-old C57BL/6J mice (both sexes) were used. Indo cyanine green (ICG) dye-labeled nanoparticle/nanocomposite formulations were nebulized using an aeroneb® lab module nebulizer in a modified closed circuit as described in the literature [91]. Saline solution nebulization was used as a negative control. The special apparatus with closed circuit will allow for filtering nanoparticles and aerosols via a HEPA filter, ensuring safety for operating personnel. ICG loaded PLGA NPs (ICG-PLGA NPs), and nanofiber coated ICG-PLGA NPs (AMNCs) were re-suspended at 2.5 mg/mL in saline for nebulization. Mice were restrained in the chamber and nebulized with various groups including saline control for 20 minutes. After nebulization, mice were monitored for any behavioral changes for an hour and euthanized for processing. Later, whole lungs were homogenized to quantify the uptake of nanoparticles and study the biodistribution. Lung tissues were rinsed with PBS and fixed in 4% paraformaldehyde at 4°C overnight and embedded with paraffin as previously described [92]. Paraffin-embedded lungs were sectioned at 5 µm thickness and stained with hematoxylin-eosin (H&E) for histological analysis.

Similarly, to visually assess nanocomposite delivery in lung tissue, coumarin-6 loaded nanoparticles and AMNCs were also used to perform *ex vivo* imaging after animal studies using Kodak *in vivo* imager (Carestream Health Inc., New Haven, CT). Briefly, after nebulization with

nanoparticles or AMNCs, the mice lungs were inflated with optimal cutting temperature compound (OCT) and dissected for further processing. Dissected lungs embedded in OCT were sectioned using a cryostat (Leica Biosystems, Germany) with a thickness of 50 μm at various regions in the lungs and stained for cell nuclei with NucBlue (Thermofisher) as previously described [93]. Microscopic slides with processed tissues were imaged using a fluorescent microscope (ECHO, San Diego) at 40x magnification.

3.3 Results & Discussion

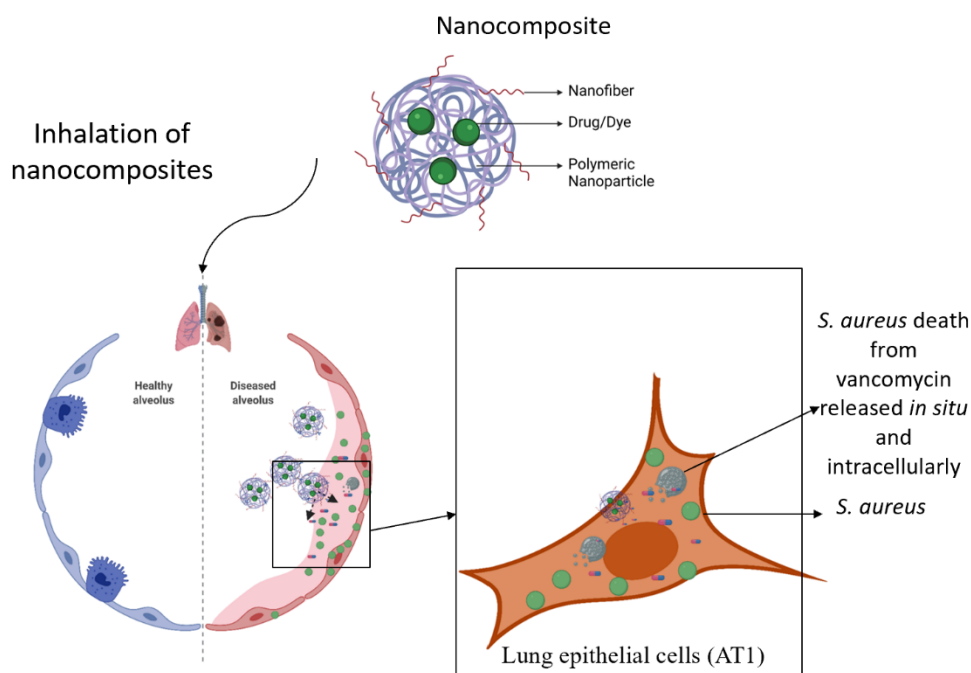


Figure 3.1 Schematic of AMNC Pulmonary Delivery and Inhibition of *S. aureus*

3.3.1 Synthesis and Characterization of AMNCs

AMNCs were prepared by combining PLGA nanoparticles and cell membrane penetrating nanofibers for enhancing drug delivery. PLGA nanoparticles were loaded with Vancomycin using a double emulsion protocol which is commonly employed to load hydrophilic antibiotics[94]. Due to the high hydrophilicity of Vancomycin and low loading efficiency found with conventional

double emulsion protocols, in our optimization process we modified the ion pairing method recently reported by Kashi et al. [94] wherein an addition of ion pairing agents such as dextran sulphate showed improvement in loading efficiency of Vancomycin from 8% to 14% by reduction of hydrophilicity of Vancomycin [94]. TEM images showed a spherical morphology (**Figure 3.2A**) and DLS showed a size distribution of Vancomycin loaded PLGA NPs (Van-PLGA NPs) around ~250-300nm. To synthesize AMNCs, Van-PLGA NPs were mixed with cell membrane penetrating nanofibers at an optimized ratio of (2 mg NPs: 0.5 mg of nanofiber) with a conjugation efficiency of 36% (Supplementary Figure).

Van-PLGA NPs with and without a nanofiber coating at physiological pH showed a biphasic drug release with initial burst release and a sustained release in PBS at 37⁰C. A nanofiber coating of Van-PLGA NPs or AMNCs showed a slightly higher rate of Vancomycin release after

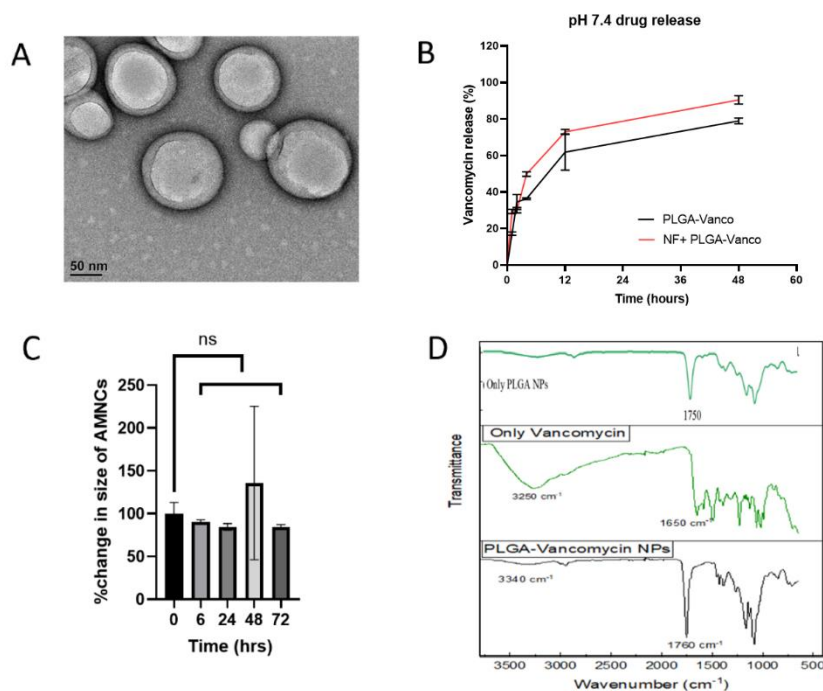


Figure 3.2 Characterization of AMNCs. **A.** TEM image of Vancomycin loaded nanoparticles. **B.** Vancomycin drug release profiles with (AMNCs) and without nanofiber coating (Van-PLGA NPs) **C.** AMNCs stability in saline showing no significance over 72 hours. **D.** FTIR showing the Vancomycin encapsulated into PLGA nanoparticles with distinct peaks of 1760 cm⁻¹ amide peaks and 3340 cm⁻¹ of -OH groups from PLGA polymer.

4 hours, but over 48 hours showed a similar amount of Vancomycin was released from both AMNCs and Van-PLGA NPs (**Figure 3.2B**). This shows that the nanofiber coating does not interfere with PLGA degradation and release of Vancomycin. More than 80% of Vancomycin is released from the nanocomposites made with low molecular weight PLGA (15-25 kDa), which is ideal for inhibition of MRSA compared to a sustained release over a long period of time leading to antibiotic resistance [95]. Additionally, AMNC stability in saline was assessed by monitoring their size and showed no significant changes over a period of 72 hours (**Figure 3.2C**). Saline stability can be translated for nebulization and other temporary storage purposes before administration.

To study the presence of functional groups of encapsulated Vancomycin in Van-PLGA NPs, FTIR was performed in a spectral range of 500-3500 cm^{-1} . Distinct amide peaks in 1760 cm^{-1} evident from the Vancomycin and -OH group peak extension at 3340 cm^{-1} was seen due to the presence of Vancomycin -OH groups added to PLGA polymer (**Figure 3.2D**).

3.3.2 Cytocompatibility of AMNCs

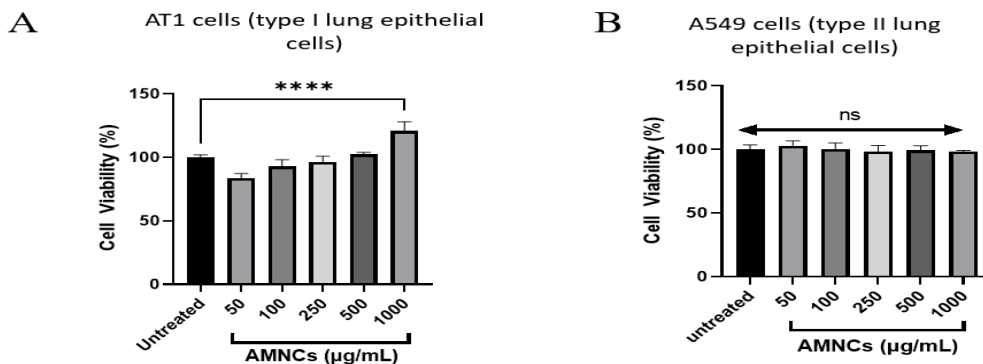


Figure 3.3 Cytocompatibility of AMNCs. MTS assay results showing the cytocompatibility of AMNCs up to 1 mg/mL in **A.** Alveolar Type 1 epithelial cells and **B.** A549 representing Alveolar Type II epithelial cells.

MTS assay results indicate that the drug loaded AMNCs showed cytocompatibility with alveolar Type 1 and A549 (Type II) epithelial cells up to 1 mg/mL following 72 hours of

incubation. More than 90% of cells in all concentrations showed viability, indicating that the AMNCs are relatively non-toxic (**Figure 3.3 A-B**). As previously reported, the nanofiber coating reduced their toxicity making AMNCs cytocompatible even with the presence of a cell membrane penetrating nanofiber coating in them (Chapter 1).

3.3.3 *In vitro* Evaluation of AMNCs Uptake in Infected Cells

Cells that undergo stress and other modifications from infections, especially MRSA infections, have shown to reduce nutrient uptake and influence growth rates [87]. AT1 cells when infected with various MOI (0.5, 1, 10, 100) of MRSA showed a reduction in nanoparticle uptake. This reduction in uptake of nanoparticles may be due to alteration in various uptake endocytosis mechanisms. PLGA is extensively studied for their drug delivery properties and improvement of a common carrier using nanofibers can offer the advantages of higher drug bioavailability and reduced dosage for treatment. Further studies investigating the effects of bacterial infections on cell uptake of nanoparticle need to be done to understand the alterations in uptake mechanisms [50]. Rhodamine B dye was replaced in AMNCs instead of Vancomycin to perform the uptake study. Compared to Rho B PLGA nanoparticles, AMNCs loaded with Rhodamine B showed significantly higher uptake at all MOI levels of MRSA infection in AT1 cells (**Figure 3.4B**). We performed a similar study in RAW macrophages with MRSA infection (MOI 1:10) with no significant change in nanoparticle uptake compared to AMNCs (data not shown here). In MRSA infected RAW cells, the uptake of NPs was comparatively higher than AT1 cells, which can be related to the phagocytic nature of macrophages. This uptake behavior may also influence uptake of nanoparticles and other modifications such as a nanofiber coating to have similar uptake seen in RAW macrophages.

To further confirm the reduced NP uptake by cells during infection, we performed flow cytometry studies. SYTO 9 (green) labeled MRSA infected AT1 cells (MOI 1:10) were given both nanoparticles and AMNCs, both loaded with Rhodamine B dye. Nanofiber coating increased the uptake of nanoparticles more than 15-fold compared to plain nanoparticles (**Figure 3.4A**). Antimicrobial peptides are promising candidates to treat infections, and novel designs of producing antimicrobial peptides/nanofiber can further improve the design of drug delivery systems such as AMNCs by having combined loading of both antibiotics and antimicrobial peptides [96].

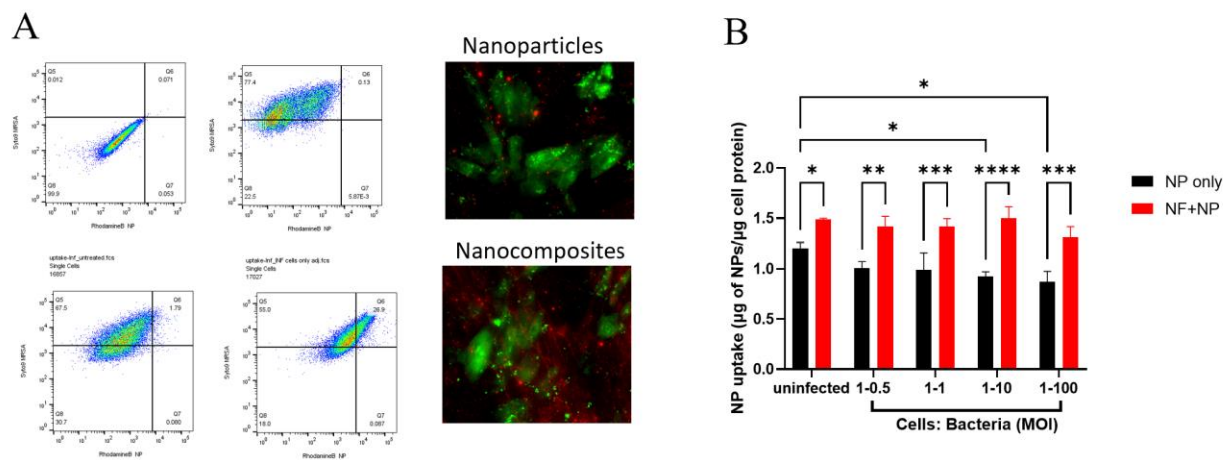


Figure 3.4 AMNC Cell Uptake in MRSA Infected AT1. **A.** Cell uptake of nanoparticles and nanocomposites measured through Flow Cytometry after 90 minutes along representative fluorescent images of the nanoparticle and nanocomposite uptake are given in the center. For this purpose, MRSA was stained with SYTO 9 (green) gated on the Y-axis and AMNC with Rhodamine B (red) gated on the X-axis on the dot plots. **B.** To quantify the AMNC uptake, AT1 cells were seeded into 24-well plates at confluency and the next day, infected with MRSA of a Multiplicity of Infection (MOI) ranging from 0.5-100. Polybrene – a transfection reagent was used as a control to enhance uptake of nanoparticles. Cells along with bacteria were spun down for 5 minutes at 2000 rpm to increase bacteria uptake by the cells. After 4 hours, cells were washed and treated with 100 µg/mL of Gentamycin for 30 minutes to remove any of the extracellular bacteria. After treatment, cells were washed and given 0.5 mg/mL of dye loaded NPs for 90 minutes. Later, cells were washed 3X with PBS and lysed using 1% Triton-X. The cell lysate was used to analyze fluoresce of NPs and protein content from the cells.

3.3.4 Antimicrobial Properties of Vancomycin Loaded Nanoparticles

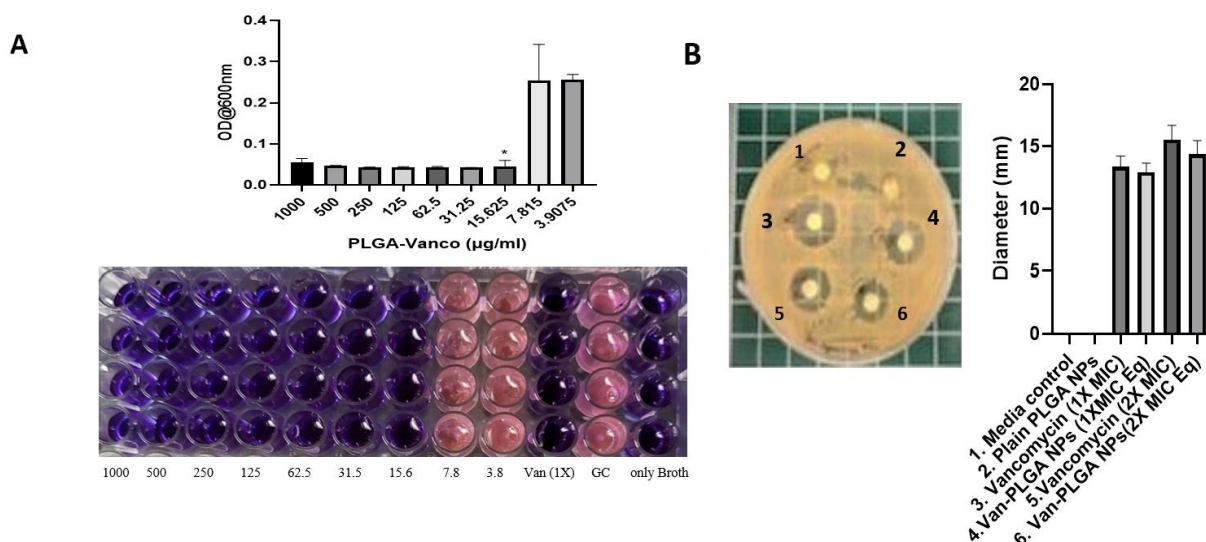


Figure 3.5 Antimicrobial effects of Van-PLGA NPs. **A.** Minimum Inhibitory Concentration study. Van-NPs were serially diluted from 500 ug/ml with positive control as free Vancomycin (1X MIC=2 ug/ml) and only media without bacteria. Bacteria without any Van-NPs served as a negative control (GC). Data in the plot was normalized against controls to determine the MIC value as indicated by the arrow in the plot. 1×10^8 CFU/ml bacteria was considered for seeding bacteria into each well. 0.015% Resazurin was added for colorimetric assessment of bacterial inhibition. (purple=bacterial inhibition, pink = bacterial growth). **B.** Zone of Inhibition. 200ul of 1×10^8 CFU/ml was plated on BHI agar plates. Sterile discs were loaded with 50 ul of samples: 1) only BHI media, 2) Plain NPs, 3) 2X MIC of free Vancomycin, 4) 1X MIC of free Vancomycin, 5) 2X MIC of Van-NPs and 6) 1X MIC of Van-NPs. Zone of Inhibition diameter was measured using ImageJ software (NIH).

To assess the antimicrobial properties of Vancomycin loaded PLGA-NPs, we performed MIC and Zone of Inhibition study. Vancomycin loaded into PLGA-NPs showed inhibition of MRSA in both the studies with free Vancomycin at MIC (2 µg/mL) as a control. In our MIC studies performed over 24 hours, an MIC of 15.6 µg/mL was observed, which correlated to the drug release kinetics of the nanoparticles (**Figure 3.5A**). The Zone of Inhibition study showed similar diameter for Zones of Inhibition between 1X and 2X MIC concentrations of free Vancomycin and equivalent concentrations of Van-PLGA NPs (**Figure 3.5B**). Plain PLGA NPs did not show any inhibition of MRSA bacteria on the plates.

3.3.5 Intracellular MRSA Killing Using AMNCs

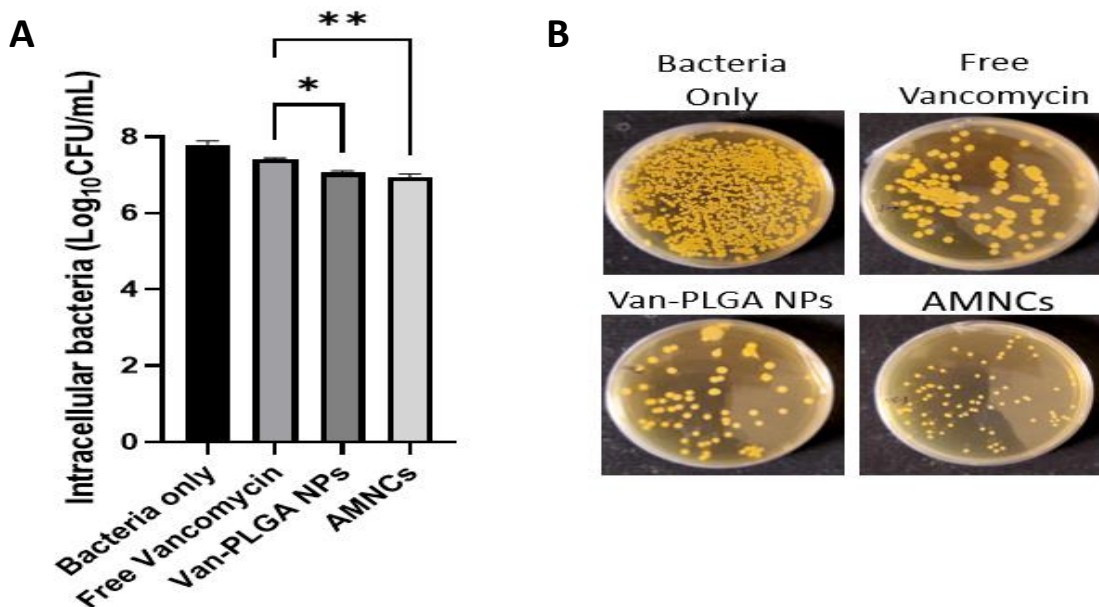


Figure 3.6 Intracellular MRSA Killing using AMNCs. 24-well plate- AT1 cells seeded at confluency MRSA given at a MOI of 10. Cells spun down to better facilitate MRSA uptake. After 3 hours, cells are treated with Gentamycin and Lysostaphin for 30 minutes to remove extracellular bacteria. Various treatments were given for 90 minutes, cells washed and incubated for 12 hours before lysis and plating on agar. After 14-18 hours, colonies were counted, and the data plotted. **A.** AMNCs showed visibly and quantitatively lower levels of intracellular bacteria implying AMNCs higher uptake and antimicrobial properties to inhibit intracellular bacteria. **B.** BHI agar plates showing the intracellular MRSA colonies after plating the cell lysate.

A MRSA bacterial infection in the lung epithelium often leads to intracellular residence, as commonly seen in alveolar macrophages causing persistent infections in lungs [21, 97]. We coated the Van-PLGA NPs with novel cell membrane penetrating nanofibers to assess the enhanced antibiotic delivery. Cell lysate from AT1 cells infected with MRSA showed reduction in bacterial burden in Vancomycin groups. Out of all the Vancomycin groups, AMNCs showed a higher inhibition of intracellular MRSA compared to Van-PLGA NPs without a nanofiber coating or the free Vancomycin groups. Gentamycin treatment of infected cells before giving any treatments ensured removing extracellular bacteria and focusing the treatments on the intracellular MRSA. After 12 hours of incubation with nanoparticles, AMNCs and free Vancomycin showed that the higher uptake ability of AMNCs can improve the antibiotic payload delivery in infected cells evident from the reduction in MRSA colonies from cell lysate (**Figure 3.6A**). Further testing

of AMNCs for their dose-dependent and time-dependent killing can improve the optimization for a therapeutic dosage. We performed a similar study where we nebulized Van-PLGA NPs and AMNCs to see the effect of the nanofiber coating. AMNCs reduced the intracellular bacteria with over one log reduction compared to Van-PLGA NPs. These results show that nebulization of AMNCs do not hinder the enhanced uptake abilities of AMNCs, evident by the increased killing of MRSA (**Figure 3.6B**).

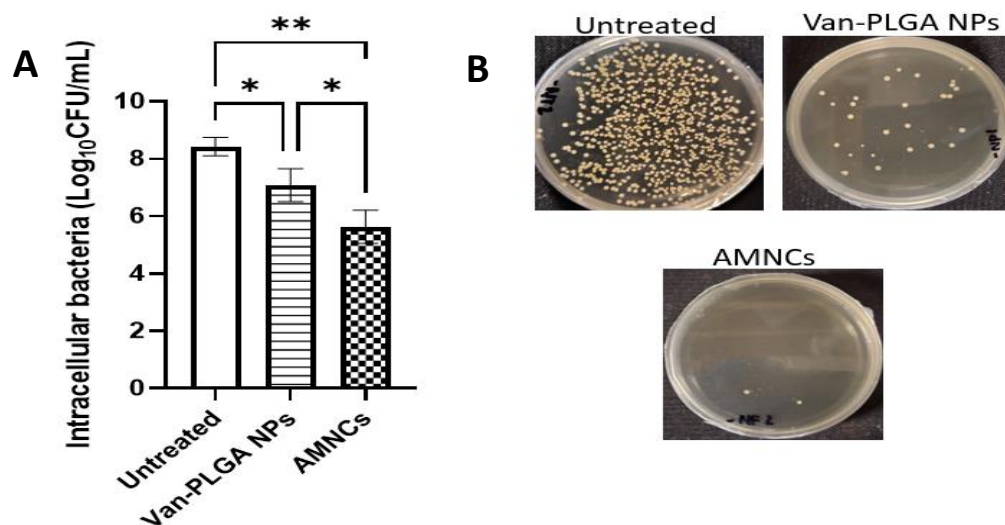


Figure 3.7 AMNCs Nebulization to Inhibit Intracellular MRSA. 24-well plate- AT1 cells were seeded at confluency. MRSA given at an MOI of 10. Cells were spun down to better facilitate MRSA uptake. After 3 hours, cells are treated with Gentamycin and Lysostaphin for 30 minutes to remove extracellular bacteria. Various treatments incubated with infected cells for 12 hours, cells washed before lysis and plated on agar. After 14-18 hours, colonies were counted, and the data plotted. **A.** AMNCs showed visibly and quantitatively lower levels of intracellular bacteria showing AMNCs higher uptake and antimicrobial properties to inhibit intracellular bacteria. **B.** BHI agar plates showing the intracellular MRSA colonies after plating the cell lysate.

3.3.6 *In Vivo* Biodistribution

The nanofibers coating of ICG-PLGA NPs was used to represent AMNCs in the biodistribution studies. The closed-circuit setup employed was adjusted for optimized uptake of nebulized particles including nanoparticles, AMNCs, liposomes or other aerosolized nanocarriers (**Figure 3.8**). Here ICG-loaded nanoparticles and AMNCs were successfully delivered via inhalation as

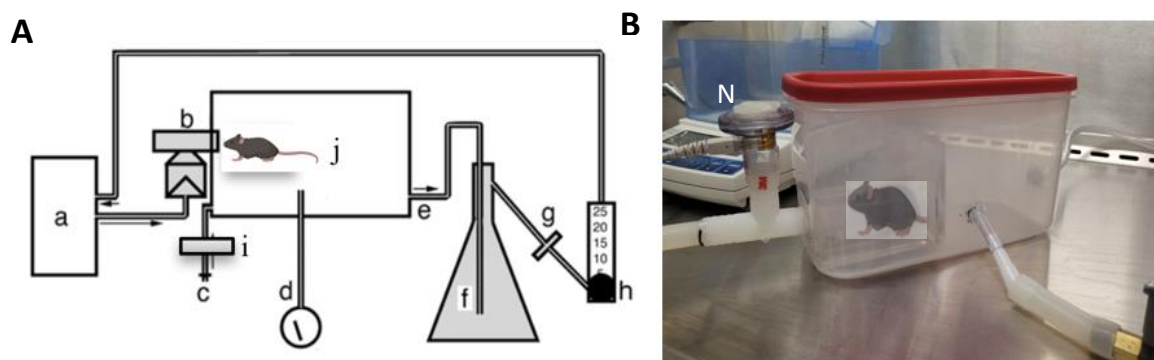


Figure 3.8 Setup of Inhalation Delivery of Nebulized ICG-PLGA NPs and AMNCs in Mice. **A.** Graphical view of modified nebulizer setup for inhalable delivery with different components: a. pump system, b. lab module nebulizer, c. clean replacement air, d. air pressure gauge, e. port to draw aerosol, f. vacuum flask, g. 0.2 μ m HEPA filter, h. air flow regulator, i. HEPA filter for clean air intake, j. mice restrainer for inhalation through nebulizer. **B.** Actual setup with nebulizer and cartoon mice restrained for inhalation of aerosols generated by the nebulizer seen by the fluorescence *ex vivo* images of lungs. Over 33% of AMNCs were delivered to the lungs via inhalation in comparison to ~7% of nanoparticles (without nanofiber coating) over an hour after nebulization (**Figures 3.9A-B**). The higher accumulation of AMNCs can be explained by the nanofiber ability to improve cell uptake and traverse the mucus layer comparatively faster as shown previously in *in vitro* studies (**Figures 2.4 & 2.6**). PLGA NPs of similar size were already shown to be deposited in the alveoli immediately after inhalation delivery. Overall negatively charged PLGA NPs were reported to be delivered to alveolar ducts compared to positively charged porous PLGA seen more in trachea, bronchia and bronchioles [98]. Pathological evaluation of H&E-stained lung tissue of PLGA NPs and AMNCs revealed mild to negligible changes when compared to the saline control (**Figure 3.9C**). No collapse of alveolar space or widened or thickened alveolar septum is visible in AMNCs or PLGA NPs. H&E images also show that mild inflammatory exudates seen in both groups is from the introduction of nanoparticles. AMNCs and PLGA NPs show similar tissue histology indicating that a nanofiber coating does not introduce any additional toxicities or changes, making it suitable for coating nanocarriers for pulmonary drug delivery.

AMNC biodistribution was also studied using Coumarin-6 dye-loaded nanoparticles. Coumarin-6 dye was used because of its superior fluorescence compared to NIR ICG dye for fluorescent microscopy purposes. To further assess the AMNC biodistribution, OCT embedded mice lungs of AMNCS or nanoparticle treatment were imaged. Fluorescent images show that Coumarin-6 AMNCs were localized along with DAPI stained nucleus (**Figure 3.10A**) and higher AMNC accumulation compared to that of nanoparticle groups (**Figure 3.10B**). These

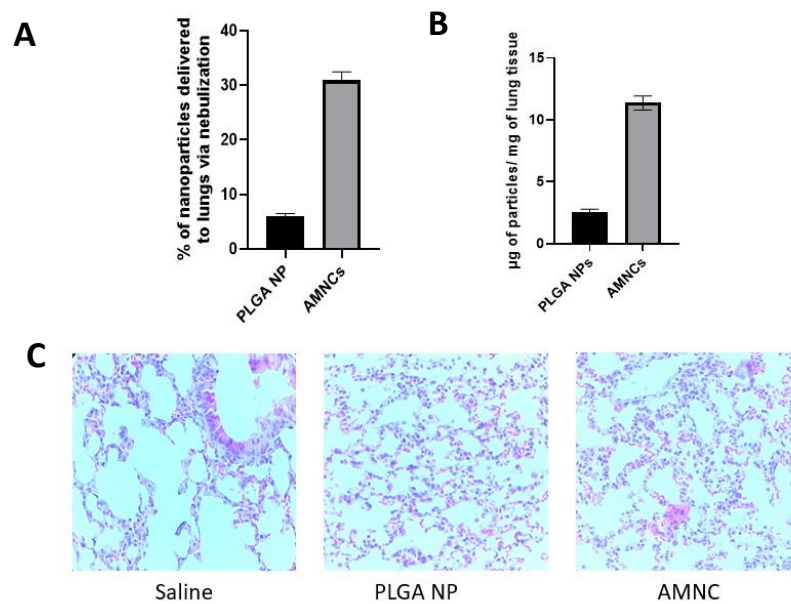


Figure 3.9 Biodistribution and H&E Staining of Lung Tissues for PLGA NPs and Nanocomposites Treatment via Nebulization in Mice. **A.** % of AMNCs delivered to mice lungs via nebulization of 7.5 mg of particles at a concentration of 2.5 mg/mL. **B.** Amount of AMNCs and PLGA NPs accumulated in the mice tissues in µg/mg. **C.** Hemoxilyn and eosin staining of paraffin-embedded lung tissues. Mild to negligible inflammation was seen in PLGA NPs and AMNCs uptaken in lung tissues compared to the control saline group (40x magnification).

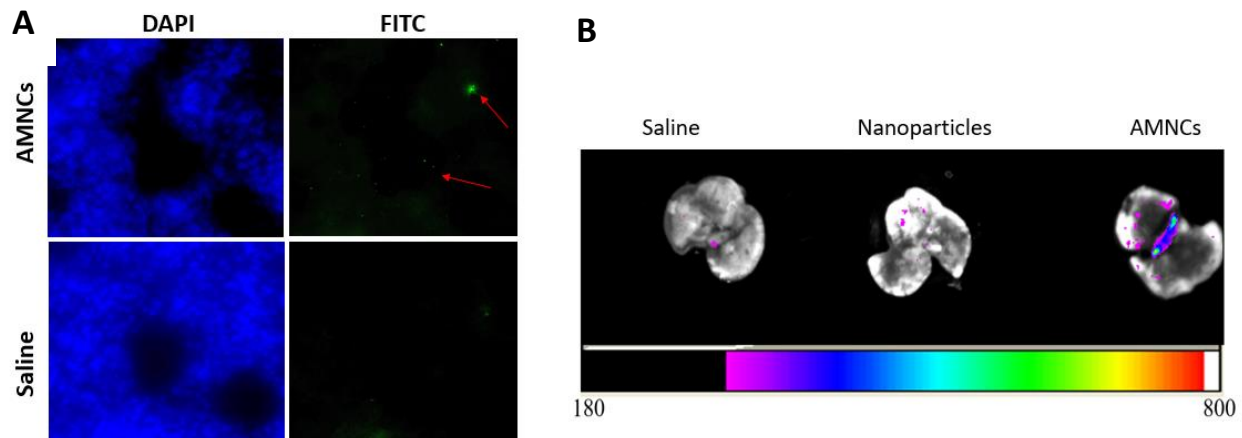


Figure 3.10 Biodistribution of Coumarin-6 Dye-Loaded AMNCs in Mice Lungs. **A.** AMNC or saline nebulized lungs were inflated and sectioned at 50 μm thickness, and then stained with Nucblue for the nucleus. Fluorescent images show Coumarin-6 AMNCs (highlighted with red arrows) localized with DAPI stained nuclei of cells in lung tissue (40x magnification). **B.** After nebulizing saline, Coumarin-6 dye-loaded nanoparticles and AMNCs from lungs from mice were excised and imaged for distribution of particles. AMNCs show higher distribution in lung tissues compared to those of nanoparticles.

results indicate that AMNCs nebulized and inhaled by the mice were able to reach the alveolar region and are retained at a higher number compared to nanoparticles without any nanofiber coating. Overall, biodistribution studies show that nanofiber coating onto nanoparticles is safe and enhances delivery of nanoparticles.

3.4 Conclusion

In this study, the antimicrobial drug Vancomycin was successfully loaded into PLGA NPs at a higher loading efficiency of >14% compared to the other literature via an ion-pairing method and double emulsion protocol [99]. Novel AMNCs was synthesized with abilities of enhanced drug delivery and applied as a drug carrier to inhibit MRSA infection in primary lung alveolar epithelial cells. Nanofiber coated AMNCs showed higher uptake in infected cells compared to PLGA NPs, demonstrating their potential to deliver potent antimicrobials to infected cells with high cytocompatibility. AMNCs were able to inhibit intracellular MRSA either given directly in

media or via nebulization with an increased potency compared with nanoparticles alone due to their higher affinity for uptake. *In vivo* biodistribution of AMNCs showed a 3-fold higher accumulation in the lungs compared to nanoparticles without a nanofiber coating. Together, these characteristics indicate that the AMNCs have potential application for treating MRSA lung infections through the route of administration by inhalation and can also be applied towards other lung infections with their ability to load various payloads, including different antimicrobials.

Chapter 4

CONCLUSIONS AND FUTURE WORK

4.1 Conclusions

To summarize, a novel nanocomposite was developed with the capability to load antibiotics for pulmonary drug delivery to treat lung infections effectively. The second chapter involves the synthesis and characterization of nanocomposites made from a coating of cell membrane penetrating nanofiber onto PLGA NPs for enhanced pulmonary delivery of drugs for inhalation purposes. The nanocomposites showed promise in terms of optimal size ~200 nm and saline stability suitable for lung inhalation [80], and *in vitro* cytocompatibility with reduction in the toxicity of nanofibers, which are found toxic at higher concentrations when uncoated. Additionally, the nanocomposites maintained the coating of the nanofiber which is evident from the enhanced uptake ability in lung epithelial cells even after freeze-drying and nebulization. This shows the translative potential of a nanofiber coating for enhancing drug delivery via improved nanoparticle cellular uptake.

Pathological conditions such as lung infections can lead to altered cellular uptake mechanisms in infected cells as seen in lung epithelial cells [87]. Based on the results of our novel nanocomposites showing enhanced drug delivery, we modified the nanocomposites to load Vancomycin and used them to treat MRSA infected lung epithelial cells. Our nanocomposites formulated with Vancomycin drug payload showed improved intracellular MRSA killing in lung epithelial cells both by incubation in media and nebulized delivery, owing to the abilities of nanofiber coating to improve uptake of nanocomposites in healthy as well as diseased cells. These results support our hypothesis that nanofiber coatings on drug carriers can improve their uptake in

diseased cells, increasing drug accumulation and eventually enhancing therapeutic efficacy of potent drugs for inhalation delivery in lungs.

4.2 Limitations

Although our findings show improvement in inhalation delivery of nanocarriers, some limitations still exist which need to be addressed and are detailed below. Nanofibers used in our project do not have a specific cell targeting ability, which limits the use of our nanocomposites for inhalable drug delivery. One major limitation observed in chapter 2 is that the optimization of nanofiber and nanoparticle ratio, which depends on the surface charge of the nanoparticles, needs to be further investigated. A relationship between zeta potential of nanoparticle surface and amount of nanofiber that can be coated needs to be established. This information can help understand the amount of nanofiber coating needed for optimal enhancement of nanoparticle uptake.

Also, the loading of the drug can alter the surface charge of nanoparticles, especially polymer nanoparticles, altering the coating ability of nanofibers which may reduce the uptake efficiency. Studying the effects of drug loading on correlation with nanofiber coating can optimize the final formulations. Another limitation associated with drug loading is the pre-mature release of the drug while coating of the nanofiber, which is evident in highly hydrophilic drugs, reducing the therapeutic efficiency of the nanocomposite system. Use of a high molecular weight polymer or ion pairing methods to reduce hydrophilicity of drugs can lower the premature drug release.

4.3 Outlook

Based on our encouraging results, future therapeutic studies in mice models with MRSA lung infections with various dosages should be performed to assess the optimal dose and clinical potential of antimicrobial nanocomposites. Future studies, including toxicity studies and/or

survival studies with severe infections, can be helpful to understand the pharmacokinetics and pharmacodynamics of nanocomposites in infected mice. Use of imaging agents such as fluorescent dyes or metal-based nanoparticles encapsulated into nanocomposites may improve imaging to understand the physiology of lower respiratory lung tissue in diseased conditions.

Targeted peptide coating of nanocarriers have shown promise in targeting specific cells or tissue for delivery of therapeutics [48, 61]. Nanofibers with targeting moieties can be used to improve the targeting while maintaining the enhanced cellular uptake of nanocomposites. These strategies of multifunctional nanocarriers can open new avenues in the treatment of diseases like cancer as well as inflammatory diseases like cardiovascular disease, peripheral artery disease, among others which utilize IV administration of drug delivery. Along with antimicrobials, various other payloads such as small molecule drugs, siRNA, mRNA, plasmid DNA and proteins can be loaded into nanocomposites for enhanced drug delivery for the treatment of lung infections. With the recent success of nanotechnology-enabled drug carriers, the field of nanomedicine has grown exponentially in treatment of various pathologies. The novel nanocomposites presented in this work hold promise as an enhanced drug delivery platform for several clinical applications.

References

- [1] J.F. Murray, The structure and function of the lung [Review article. 2010: The Year of the Lung. Series editor: John F. Murray], *The International Journal of Tuberculosis and Lung Disease* 14(4) (2010) 391-396.
- [2] E.A. Oczypok, T.N. Perkins, T.D. Oury, Alveolar Epithelial Cell-Derived Mediators: Potential Direct Regulators of Large Airway and Vascular Responses, *Am J Respir Cell Mol Biol* 56(6) (2017) 694-699.
- [3] Y. Wang, Z. Tang, H. Huang, J. Li, Z. Wang, Y. Yu, C. Zhang, J. Li, H. Dai, F. Wang, T. Cai, N. Tang, Pulmonary alveolar type I cell population consists of two distinct subtypes that differ in cell fate, *Proceedings of the National Academy of Sciences* 115(10) (2018) 2407-2412.
- [4] T.J. Desai, D.G. Brownfield, M.A. Krasnow, Alveolar progenitor and stem cells in lung development, renewal and cancer, *Nature* 507(7491) (2014) 190-4.
- [5] B.D. Uhal, Cell cycle kinetics in the alveolar epithelium, *American Journal of Physiology-Lung Cellular and Molecular Physiology* 272(6) (1997) L1031-L1045.
- [6] Z.C. Chroneos, Z. Sever-Chroneos, V.L. Shepherd, Pulmonary Surfactant: An Immunological Perspective, *Cellular Physiology and Biochemistry* 25(1) (2010) 13-26.
- [7] K. Yamamoto, J.D. Ferrari, Y. Cao, M.I. Ramirez, M.R. Jones, L.J. Quinton, J.P. Mizgerd, Type I Alveolar Epithelial Cells Mount Innate Immune Responses during Pneumococcal Pneumonia, *The Journal of Immunology* 189(5) (2012) 2450.
- [8] A.J. Thorley, D. Grandolfo, E. Lim, P. Goldstraw, A. Young, T.D. Tetley, Innate Immune Responses to Bacterial Ligands in the Peripheral Human Lung – Role of Alveolar Epithelial TLR Expression and Signalling, *PLOS ONE* 6(7) (2011) e21827.
- [9] J.P. Mizgerd, Lung Infection—A Public Health Priority, *PLOS Medicine* 3(2) (2006) e76.
- [10] C. Troeger, B. Blacker, I.A. Khalil, P.C. Rao, J. Cao, S.R.M. Zimsen, S.B. Albertson, A. Deshpande, T. Farag, Z. Abebe, I.M.O. Adetifa, T.B. Adhikari, M. Akibu, F.H. Al Lami, A. Al-Eyadhy, N. Alvis-Guzman, A.T. Amare, Y.A. Amoako, C.A.T. Antonio, O. Aremu, E.T. Asfaw, S.W. Asgedom, T.M. Atey, E.F. Attia, E.F.G.A. Avokpaho, H.T. Ayele, T.B. Ayuk, K. Balakrishnan, A. Barac, Q. Bassat, M. Behzadifar, M. Behzadifar, S. Bhaumik, Z.A. Bhutta, A. Bijani, M. Brauer, A. Brown, P.A.M. Camargos, C.A. Castañeda-Orjuela, D. Colombara, S. Conti, A.F. Dadi, L. Dandona, R. Dandona, H.P. Do, E. Dubljanin, D. Edessa, H. Elkout, A.Y. Endries, D.O. Fijabi, K.J. Foreman, M.H. Forouzanfar, N. Fullman, A.L. Garcia-Basteiro, B.D. Gessner, P.W. Gething, R. Gupta, T. Gupta, G.B. Hailu, H.Y. Hassen, M.T. Hedayati, M. Heidari, D.T. Hibstu, N. Horita, O.S. Ilesanmi, M.B. Jakovljevic, A.A. Jamal, A. Kahsay, A. Kasaeian, D.H. Kassa, Y.S. Khader, E.A. Khan, M.N. Khan, Y.-H. Khang, Y.J. Kim, N. Kisson, L.D. Knibbs, S. Kochhar, P.A. Koul, G.A. Kumar, R. Lodha, H. Magdy Abd El Razek, D.C. Malta, J.L. Mathew, D.T. Mengistu, H.B. Mezgebe, K.A. Mohammad, M.A. Mohammed, F. Momeniha, S. Murthy, C.T. Nguyen, K.R. Nielsen, D.N.A. Ningrum, Y.L. Nirayo, E. Oren, J.R. Ortiz, M. Pa, M.J. Postma, M. Qorbani, R. Quansah, R.K. Rai, S.M. Rana, C.L. Ranabhat, S.E. Ray, M.S. Rezai, G.M. Ruhago, S. Safiri, J.A. Salomon, B. Sartorius, M. Savic, M. Sawhney, J. She, A. Sheikh, M.S. Shiferaw, M. Shigematsu, J.A. Singh, R. Somayaji, J.D. Stanaway, M.B. Sufiyan, G.R. Taffere, M.-H. Temsah, M.J. Thompson, R. Tobe-Gai, R. Topor-Madry, B.X. Tran, T.T. Tran, K.B. Tuem, K.N. Ukwaja, S.E. Vollset, J.L. Walson, F. Weldegebreal, A. Werdecker, T.E. West, N. Yonemoto, M.E.S. Zaki, L. Zhou, S. Zodpey, T. Vos, M. Naghavi, S.S. Lim, A.H. Mokdad, C.J.L. Murray, S.I. Hay, R.C. Reiner, Jr., Estimates of the global, regional, and national morbidity, mortality, and aetiologies of lower respiratory infections in 195 countries, 1990–2016: a systematic analysis for the Global Burden of Disease Study 2016, *The Lancet Infectious Diseases* 18(11) (2018) 1191-1210.
- [11] W.O.C.M. Cookson, M.J. Cox, M.F. Moffatt, New opportunities for managing acute and chronic lung infections, *Nature Reviews Microbiology* 16(2) (2018) 111-120.
- [12] T. Ferkol, D. Schraufnagel, The global burden of respiratory disease, (2325-6621 (Electronic)).

- [13] American Lung Association, Research and Program Services, Epidemiology and Statistics Unit. Trends in pneumonia and influenza morbidity and mortality, 2010.
- [14] A.M. Smith, J.A. McCullers, Secondary bacterial infections in influenza virus infection pathogenesis, (0070-217X (Print)).
- [15] D.E. Morris, D.W. Cleary, S.C. Clarke, Secondary Bacterial Infections Associated with Influenza Pandemics, *Front Microbiol* 8 (2017) 1041-1041.
- [16] L.M. Napolitano, M.E. Brunsvold, R.C. Reddy, R.C. Hyzy, Community-acquired methicillin-resistant *Staphylococcus aureus* pneumonia and ARDS: 1-year follow-up, (1931-3543 (Electronic)).
- [17] S.N. Qazi, J. Council E Fau - Morrissey, C.E. Morrissey J Fau - Rees, A. Rees Ce Fau - Cockayne, K. Cockayne A Fau - Winzer, W.C. Winzer K Fau - Chan, P. Chan Wc Fau - Williams, P.J. Williams P Fau - Hill, P.J. Hill, agr expression precedes escape of internalized *Staphylococcus aureus* from the host endosome, (0019-9567 (Print)).
- [18] B. Giese, K. Glowinski F Fau - Paprotka, S. Paprotka K Fau - Dittmann, T. Dittmann S Fau - Steiner, B. Steiner T Fau - Sinha, M.J. Sinha B Fau - Fraunholz, M.J. Fraunholz, Expression of δ -toxin by *Staphylococcus aureus* mediates escape from phago-endosomes of human epithelial and endothelial cells in the presence of β -toxin, (1462-5822 (Electronic)).
- [19] K.W. Bayles, L.E. Wesson Ca Fau - Liou, L.K. Liou Le Fau - Fox, G.A. Fox Lk Fau - Bohach, W.R. Bohach Ga Fau - Trumble, W.R. Trumble, Intracellular *Staphylococcus aureus* escapes the endosome and induces apoptosis in epithelial cells, (0019-9567 (Print)).
- [20] M. Kubica, J. Guzik K Fau - Koziel, M. Koziel J Fau - Zarebski, W. Zarebski M Fau - Richter, B. Richter W Fau - Gajkowska, A. Gajkowska B Fau - Golda, A. Golda A Fau - Maciag-Gudowska, K. Maciag-Gudowska A Fau - Brix, L. Brix K Fau - Shaw, T. Shaw L Fau - Foster, J. Foster T Fau - Potempa, J. Potempa, A potential new pathway for *Staphylococcus aureus* dissemination: the silent survival of *S. aureus* phagocytosed by human monocyte-derived macrophages, (1932-6203 (Electronic)).
- [21] D. Parker, A. Prince, Immunopathogenesis of *Staphylococcus aureus* pulmonary infection, *Seminars in Immunopathology* 34(2) (2012) 281-297.
- [22] S. Esposito, G. Pennoni, V. Mencarini, N. Palladino, L. Peccini, N. Principi, Antimicrobial Treatment of *Staphylococcus aureus* in Patients With Cystic Fibrosis, *Frontiers in Pharmacology* 10 (2019).
- [23] F.J. Martin, D.M. Gomez Mi Fau - Wetzel, G. Wetzel Dm Fau - Memmi, M. Memmi G Fau - O'Seaghdha, G. O'Seaghdha M Fau - Soong, C. Soong G Fau - Schindler, A. Schindler C Fau - Prince, A. Prince, *Staphylococcus aureus* activates type I IFN signaling in mice and humans through the Xr repeated sequences of protein A, (1558-8238 (Electronic)).
- [24] D.M. Bamberger, S.E. Boyd, Management of *Staphylococcus aureus* infections, *Am Fam Physician* 72(12) (2005) 2474-81.
- [25] Guidelines for the Management of Adults with Hospital-acquired, Ventilator-associated, and Healthcare-associated Pneumonia, *American Journal of Respiratory and Critical Care Medicine* 171(4) (2005) 388-416.
- [26] M.J. Rybak, L.M. Albrecht, S.C. Boike, P.H. Chandrasekar, Nephrotoxicity of vancomycin, alone and with an aminoglycoside, *Journal of Antimicrobial Chemotherapy* 25(4) (1990) 679-687.
- [27] A. Forouzesh, P.A. Moise, G. Sakoulas, Vancomycin Ototoxicity: a Reevaluation in an Era of Increasing Doses, *Antimicrobial Agents and Chemotherapy* 53(2) (2009) 483-486.
- [28] M.Z. Rahman Sabuj, N. Islam, Inhaled antibiotic-loaded polymeric nanoparticles for the management of lower respiratory tract infections, *Nanoscale Advances* 3(14) (2021) 4005-4018.
- [29] F. Andrade, D. Rafael, M. Videira, D. Ferreira, A. Sosnik, B. Sarmento, Nanotechnology and pulmonary delivery to overcome resistance in infectious diseases, *Adv Drug Deliv Rev* 65(13-14) (2013) 1816-1827.
- [30] V. Monteil, H. Kwon, P. Prado, A. Hagelkrüys, R.A. Wimmer, M. Stahl, A. Leopoldi, E. Garreta, C. Hurtado del Pozo, F. Prosper, J.P. Romero, G. Wirnsberger, H. Zhang, A.S. Slutsky, R. Conder, N.

- Montserrat, A. Mirazimi, J.M. Penninger, Inhibition of SARS-CoV-2 Infections in Engineered Human Tissues Using Clinical-Grade Soluble Human ACE2, *Cell* 181(4) (2020) 905-913.e7.
- [31] G. Oberdörster, J. Oberdörster E Fau - Oberdörster, J. Oberdörster, Nanotoxicology: an emerging discipline evolving from studies of ultrafine particles, (0091-6765 (Print)).
- [32] H. Qiao, W. Liu, H. Gu, D. Wang, Y. Wang, The Transport and Deposition of Nanoparticles in Respiratory System by Inhalation, *Journal of Nanomaterials* 2015 (2015) 394507.
- [33] T. Kato, Y. Yashiro T Fau - Murata, D.C. Murata Y Fau - Herbert, K. Herbert Dc Fau - Oshikawa, M. Oshikawa K Fau - Bando, S. Bando M Fau - Ohno, Y. Ohno S Fau - Sugiyama, Y. Sugiyama, Evidence that exogenous substances can be phagocytized by alveolar epithelial cells and transported into blood capillaries, (0302-766X (Print)).
- [34] M. Doroudian, R. MacLoughlin, F. Poynton, A. Prina-Mello, S.C. Donnelly, Nanotechnology based therapeutics for lung disease, *Thorax* 74(10) (2019) 965.
- [35] S.C. Jurek, M. Hirano-Kobayashi, H. Chiang, D.S. Kohane, B.D. Matthews, Prevention of ventilator-induced lung edema by inhalation of nanoparticles releasing ruthenium red, *Am J Respir Cell Mol Biol* 50(6) (2014) 1107-1117.
- [36] C.Y. Zhang, W. Lin, J. Gao, X. Shi, M. Davaritouchae, A.E. Nielsen, R.J. Mancini, Z. Wang, pH-Responsive Nanoparticles Targeted to Lungs for Improved Therapy of Acute Lung Inflammation/Injury, *ACS Appl Mater Interfaces* 11(18) (2019) 16380-16390.
- [37] A.P.L. D'Almeida, M.T. Pacheco de Oliveira, T. de Souza É, D. de Sá Coutinho, B.T. Ciambarella, C.R. Gomes, T. Terroso, S.S. Guterres, A.R. Pohlmann, P.M. Silva, M.A. Martins, A. Bernardi, α -bisabolol-loaded lipid-core nanocapsules reduce lipopolysaccharide-induced pulmonary inflammation in mice, (1178-2013 (Electronic)).
- [38] H.X. Nguyen, Targeted Delivery of Surface-Modified Nanoparticles: Modulation of Inflammation for Acute Lung Injury, *Surface Modification of Nanoparticles for Targeted Drug Delivery* (2019) 331-353.
- [39] X. Hu, F.-F. Yang, L.-H. Quan, C.-Y. Liu, X.-M. Liu, C. Ehrhardt, Y.-H. Liao, Pulmonary delivered polymeric micelles – Pharmacokinetic evaluation and biodistribution studies, *European Journal of Pharmaceutics and Biopharmaceutics* 88(3) (2014) 1064-1075.
- [40] D.T. Pham, A. Chokamonsirikun, V. Phattaravorakarn, W. Tiyafoonchai, Polymeric micelles for pulmonary drug delivery: a comprehensive review, *Journal of Materials Science* 56(3) (2021) 2016-2036.
- [41] N. Wauthoz, K. Amighi, Phospholipids in pulmonary drug delivery, *European Journal of Lipid Science and Technology* 116(9) (2014) 1114-1128.
- [42] K.K. Gill, S. Nazzal, A. Kaddoumi, Paclitaxel loaded PEG(5000)-DSPE micelles as pulmonary delivery platform: formulation characterization, tissue distribution, plasma pharmacokinetics, and toxicological evaluation, *Eur J Pharm Biopharm* 79(2) (2011) 276-84.
- [43] M. Rudokas, M. Najlah, M.A. Alhnan, A. Elhissi, Liposome Delivery Systems for Inhalation: A Critical Review Highlighting Formulation Issues and Anticancer Applications, *Medical Principles and Practice* 25(suppl 2)(Suppl. 2) (2016) 60-72.
- [44] J.U. Menon, P. Ravikumar, A. Pise, D. Gyawali, C.C.W. Hsia, K.T. Nguyen, Polymeric nanoparticles for pulmonary protein and DNA delivery, *Acta Biomaterialia* 10(6) (2014) 2643-2652.
- [45] K. Jabłczyńska, M. Janczewska, A. Kulikowska, T.R. Sosnowski, Preparation and Characterization of Biocompatible Polymer Particles as Potential Nanocarriers for Inhalation Therapy, *International Journal of Polymer Science* 2015 (2015) 763020.
- [46] J.C. Sung, B.L. Pulliam, D.A. Edwards, Nanoparticles for drug delivery to the lungs, *Trends in Biotechnology* 25(12) (2007) 563-570.
- [47] A. Sharma, S. Sharma, G.K. Khuller, Lectin-functionalized poly (lactide-co-glycolide) nanoparticles as oral/aerosolized antitubercular drug carriers for treatment of tuberculosis, *J Antimicrob Chemother* 54(4) (2004) 761-6.

- [48] W.-j. Jeong, J. Bu, L.J. Kubiatowicz, S.S. Chen, Y. Kim, S. Hong, Peptide–nanoparticle conjugates: a next generation of diagnostic and therapeutic platforms?, *Nano Convergence* 5(1) (2018) 38.
- [49] W. Gao, S. Thamphiwatana, P. Angsantikul, L. Zhang, Nanoparticle approaches against bacterial infections, *WIREs Nanomedicine and Nanobiotechnology* 6(6) (2014) 532-547.
- [50] J.J. Rennick, A.P.R. Johnston, R.G. Parton, Key principles and methods for studying the endocytosis of biological and nanoparticle therapeutics, *Nature Nanotechnology* 16(3) (2021) 266-276.
- [51] P. Foroozandeh, A.A. Aziz, Insight into Cellular Uptake and Intracellular Trafficking of Nanoparticles, *Nanoscale Research Letters* 13(1) (2018) 339.
- [52] Y. Abo-zeid, G.R. Williams, L. Touabi, G.R. McLean, An investigation of rhinovirus infection on cellular uptake of poly (glycerol-adipate) nanoparticles, *International Journal of Pharmaceutics* 589 (2020) 119826.
- [53] S.P. Newman, Drug delivery to the lungs: challenges and opportunities, *Therapeutic Delivery* 8(8) (2017) 647-661.
- [54] S.H. van Rijt, T. Bein, S. Meiners, Medical nanoparticles for next generation drug delivery to the lungs, *European Respiratory Journal* 44(3) (2014) 765-774.
- [55] Forum of International Respiratory Societies. The Global Impact of Respiratory Disease European Respiratory Society, 2017.
- [56] M.J. Mitchell, M.M. Billingsley, R.M. Haley, M.E. Wechsler, N.A. Peppas, R. Langer, Engineering precision nanoparticles for drug delivery, *Nature Reviews Drug Discovery* 20(2) (2021) 101-124.
- [57] S. Gelperina, K. Kisich, M.D. Iseman, L. Heifets, The potential advantages of nanoparticle drug delivery systems in chemotherapy of tuberculosis, *American journal of respiratory and critical care medicine* 172(12) (2005) 1487-1490.
- [58] P.J. Oh N, Endocytosis and exocytosis of nanoparticles in mammalian cells, *Int J Nanomedicine* 9 (2014) 51-63.
- [59] A. Prokop, J.M. Davidson, Nanovehicular intracellular delivery systems, *J Pharm Sci* 97(9) (2008) 3518-3590.
- [60] P. Vila-Gómez, J.E. Noble, M.G. Ryadnov, Peptide Nanoparticles for Gene Packaging and Intracellular Delivery, *Methods Mol Biol* 2208 (2021) 33-48.
- [61] M.S. Shoshan, T. Vonderach, B. Hattendorf, H. Wennemers, Peptide-Coated Platinum Nanoparticles with Selective Toxicity against Liver Cancer Cells, *Angewandte Chemie International Edition* 58(15) (2019) 4901-4905.
- [62] Z. Ma, Y. Zhang, J. Zhang, W. Zhang, M.F. Foda, X. Dai, H. Han, Ultrasmall Peptide-Coated Platinum Nanoparticles for Precise NIR-II Photothermal Therapy by Mitochondrial Targeting, *ACS Appl Mater Interfaces* 12(35) (2020) 39434-39443.
- [63] S. Yang, H. Dong, Modular design and self-assembly of multidomain peptides towards cytocompatible supramolecular cell penetrating nanofibers, *RSC Advances* 10(49) (2020) 29469-29474.
- [64] V.L. Messerschmidt, U. Chintapula, A.E. Kuriakose, S. Laboy, T.T.D. Truong, L.A. Kydd, J. Jaworski, Z. Pan, H. Sadek, K.T. Nguyen, J. Lee, Notch Intracellular Domain Plasmid Delivery via Poly(Lactic-Co-Glycolic Acid) Nanoparticles to Upregulate Notch Pathway Molecules, *Front Cardiovasc Med* 8 (2021) 707897-707897.
- [65] M. Jerabek-Willemsen, T. André, R. Wanner, H.M. Roth, S. Duhr, P. Baaske, D. Breitsprecher, MicroScale Thermophoresis: Interaction analysis and beyond, *Journal of Molecular Structure* 1077 (2014) 101-113.
- [66] R. Iyer, T. Nguyen, D. Padanilam, C. Xu, D. Saha, K.T. Nguyen, Y. Hong, Glutathione-responsive biodegradable polyurethane nanoparticles for lung cancer treatment, *Journal of Controlled Release* 321 (2020) 363-371.
- [67] B. Casciaro, I. d'Angelo, X. Zhang, M.R. Loffredo, G. Conte, F. Cappiello, F. Quaglia, Y.-P.P. Di, F. Ungaro, M.L. Mangoni, Poly(lactide-co-glycolide) Nanoparticles for Prolonged Therapeutic Efficacy of

- Esculentin-1a-Derived Antimicrobial Peptides against *Pseudomonas aeruginosa* Lung Infection: in Vitro and in Vivo Studies, *Biomacromolecules* 20(5) (2019) 1876-1888.
- [68] F. Emami, S.J. Mostafavi Yazdi, D.H. Na, Poly(lactic acid)/poly(lactic-co-glycolic acid) particulate carriers for pulmonary drug delivery, *Journal of Pharmaceutical Investigation* 49(4) (2019) 427-442.
- [69] O. Harush-Frenkel, M. Bivas-Benita, T. Nassar, C. Springer, Y. Sherman, A. Avital, Y. Altschuler, J. Borlak, S. Benita, A safety and tolerability study of differently-charged nanoparticles for local pulmonary drug delivery, *Toxicol Appl Pharmacol* 246(1-2) (2010) 83-90.
- [70] K. Ohashi, T. Kabasawa, T. Ozeki, H. Okada, One-step preparation of rifampicin/poly(lactic-co-glycolic acid) nanoparticle-containing mannitol microspheres using a four-fluid nozzle spray drier for inhalation therapy of tuberculosis, *J Control Release* 135(1) (2009) 19-24.
- [71] R. Galindo, E. Sánchez-López, M.J. Gómara, M. Espina, M. Ettcheto, A. Cano, I. Haro, A. Camins, M.L. García, Development of Peptide Targeted PLGA-PEGylated Nanoparticles Loading Licochalcone-A for Ocular Inflammation, *Pharmaceutics* 14(2) (2022) 285.
- [72] K. Saar, M. Lindgren, M. Hansen, E. Eiríksdóttir, Y. Jiang, K. Rosenthal-Aizman, M. Sassian, U. Langel, Cell-penetrating peptides: a comparative membrane toxicity study, *Anal Biochem* 345(1) (2005) 55-65.
- [73] M. Pivard, K. Moreau, F. Vandenesch, *Staphylococcus aureus* Arsenal To Conquer the Lower Respiratory Tract, *mSphere* 6(3) (2021) e00059-21.
- [74] J.P. Richard, K. Melikov, E. Vives, C. Ramos, B. Verbeure, M.J. Gait, L.V. Chernomordik, B. Lebleu, Cell-penetrating peptides. A reevaluation of the mechanism of cellular uptake, *J Biol Chem* 278(1) (2003) 585-90.
- [75] M. Zanin, P. Baviskar, R. Webster, R. Webby, The Interaction between Respiratory Pathogens and Mucus, *Cell Host & Microbe* 19(2) (2016) 159-168.
- [76] S.K. Lai, Y.-Y. Wang, J. Hanes, Mucus-penetrating nanoparticles for drug and gene delivery to mucosal tissues, *Adv Drug Deliv Rev* 61(2) (2009) 158-171.
- [77] S. Hua, M.B.C. de Matos, J.M. Metselaar, G. Storm, Current Trends and Challenges in the Clinical Translation of Nanoparticulate Nanomedicines: Pathways for Translational Development and Commercialization, *Frontiers in Pharmacology* 9 (2018).
- [78] J.C. Horstmann, C.R. Thorn, P. Carius, F. Graef, X. Murgia, C. de Souza Carvalho-Wodarz, C.-M. Lehr, A Custom-Made Device for Reproducibly Depositing Pre-metered Doses of Nebulized Drugs on Pulmonary Cells in vitro, *Frontiers in Bioengineering and Biotechnology* 9 (2021).
- [79] C. Liu, A. Bayer, S.E. Cosgrove, R.S. Daum, S.K. Fridkin, R.J. Gorwitz, S.L. Kaplan, A.W. Karchmer, D.P. Levine, B.E. Murray, M.J. Rybak, D.A. Talan, H.F. Chambers, Clinical Practice Guidelines by the Infectious Diseases Society of America for the Treatment of Methicillin-Resistant *Staphylococcus aureus* Infections in Adults and Children, *Clinical Infectious Diseases* 52(3) (2011) e18-e55.
- [80] G. Kaur, R.K. Narang, G. Rath, A.K. Goyal, *Advances in Pulmonary Delivery of Nanoparticles, Artificial Cells, Blood Substitutes, and Biotechnology* 40(1-2) (2012) 75-96.
- [81] R. Yang, S.G. Yang, W.S. Shim, F. Cui, G. Cheng, I.W. Kim, D.D. Kim, S.J. Chung, C.K. Shim, Lung-specific delivery of paclitaxel by chitosan-modified PLGA nanoparticles via transient formation of microaggregates, *J Pharm Sci* 98(3) (2009) 970-84.
- [82] J.-Z. Wu, G.R. Williams, H.-Y. Li, D.-X. Wang, S.-D. Li, L.-M. Zhu, Insulin-loaded PLGA microspheres for glucose-responsive release, *Drug Delivery* 24(1) (2017) 1513-1525.
- [83] R. Pandey, A. Sharma, A. Zahoor, S. Sharma, G.K. Khuller, B. Prasad, Poly (DL-lactide-co-glycolide) nanoparticle-based inhalable sustained drug delivery system for experimental tuberculosis, *J Antimicrob Chemother* 52(6) (2003) 981-6.
- [84] J.C. Sung, D.J. Padilla, L. Garcia-Contreras, J.L. Verberkmoes, D. Durbin, C.A. Peloquin, K.J. Elbert, A.J. Hickey, D.A. Edwards, Formulation and pharmacokinetics of self-assembled rifampicin nanoparticle systems for pulmonary delivery, *Pharm Res* 26(8) (2009) 1847-55.

- [85] R. Trivedi, E.F. Redente, A. Thakur, D.W. Riches, U.B. Kompella, Local delivery of biodegradable pirfenidone nanoparticles ameliorates bleomycin-induced pulmonary fibrosis in mice, *Nanotechnology* 23(50) (2012) 505101.
- [86] B. Sinha, B. Mukherjee, G. Pattnaik, Poly-lactide-co-glycolide nanoparticles containing voriconazole for pulmonary delivery: in vitro and in vivo study, *Nanomedicine* 9(1) (2013) 94-104.
- [87] P. Gierok, M. Harms, K. Methling, F. Hochgräfe, M. Lalk, Staphylococcus aureus Infection Reduces Nutrition Uptake and Nucleotide Biosynthesis in a Human Airway Epithelial Cell Line, *Metabolites* 6(4) (2016) 41.
- [88] J. Kang, M.J. Dietz, K. Hughes, M. Xing, B. Li, Silver nanoparticles present high intracellular and extracellular killing against Staphylococcus aureus, *The Journal of antimicrobial chemotherapy* 74(6) (2019) 1578-1585.
- [89] A. Lacoma, L. Usón, G. Mendoza, V. Sebastián, E. Garcia-Garcia, B. Muriel-Moreno, J. Domínguez, M. Arruebo, C. Prat, Novel intracellular antibiotic delivery system against Staphylococcus aureus: cloxacillin-loaded poly(d,l-lactide-co-glycolide) acid nanoparticles, *Nanomedicine* 15(12) (2020) 1189-1203.
- [90] L. Di Cristo, C.M. Maguire, K. Mc Quillan, M. Aleardi, Y. Volkov, D. Movia, A. Prina-Mello, Towards the Identification of an In Vitro Tool for Assessing the Biological Behavior of Aerosol Supplied Nanomaterials, *Int J Environ Res Public Health* 15(4) (2018) 563.
- [91] W.G. Schroeder, L.M. Mitrescu, M.L. Hart, R. Unnithan, J.M. Gilchrist, E.E. Smith, C. Shanley, K.M. Benedict, L. Taraba, J. Volckens, R.J. Basaraba, A.R. Schenkel, Flexible low-cost system for small animal aerosol inhalation exposure to drugs, proteins, inflammatory agents, and infectious agents, *BioTechniques* 46(3S) (2009) Piii-Pviii.
- [92] L. Hinkle, D. Le, T. Nguyen, V. Tran, C.E. Amankwa, C. Weston, H. Shen, K.T. Nguyen, M. Rahimi, S. Acharya, Nano encapsulated novel compound SA-10 with therapeutic activity in both acute and chronic murine hindlimb ischemia models, *Nanomedicine* 35 (2021) 102400.
- [93] M.K. Khang, A.E. Kuriakose, T. Nguyen, C.M.-D. Co, J. Zhou, T.T.D. Truong, K.T. Nguyen, L. Tang, Enhanced Endothelial Cell Delivery for Repairing Injured Endothelium via Pretargeting Approach and Bioorthogonal Chemistry, *ACS Biomaterials Science & Engineering* 6(12) (2020) 6831-6841.
- [94] T.s. JafarzadehJafarzadeh kashi, S. Eskandarion, M. Esfandyari-Manesh, S.M. Amin Marashi, N. Samadi, S.M. Fatemi, F. Atyabi, S. Eshraghi, R. Dinarvand, Improved drug loading and antibacterial activity of minocycline-loaded PLGA nanoparticles prepared by solid/oil/water ion pairing method, *International journal of nanomedicine* 7 (2012) 221-34.
- [95] A. Cano, M. Ettcheto, M. Espina, A. López-Machado, Y. Cajal, F. Rabanal, E. Sánchez-López, A. Camins, M.L. García, E.B. Souto, State-of-the-art polymeric nanoparticles as promising therapeutic tools against human bacterial infections, *Journal of Nanobiotechnology* 18(1) (2020) 156.
- [96] M.E. van Gent, M. Ali, P.H. Nibbering, S.N. Kłodzińska, Current Advances in Lipid and Polymeric Antimicrobial Peptide Delivery Systems and Coatings for the Prevention and Treatment of Bacterial Infections, *Pharmaceutics* 13(11) (2021) 1840.
- [97] M.C. da Silva, J.M. Zahm, D. Gras, O. Bajolet, M. Abely, J. Hinnrasky, M. Milliot, M.C. de Assis, C. Hologne, N. Bonnet, M. Merten, M.C. Plotkowski, E. Puchelle, Dynamic interaction between airway epithelial cells and Staphylococcus aureus, *Am J Physiol Lung Cell Mol Physiol* 287(3) (2004) L543-51.
- [98] F. Ungaro, I. d'Angelo, C. Coletta, R. d'Emmanuele di Villa Bianca, R. Sorrentino, B. Perfetto, M.A. Tufano, A. Miro, M.I. La Rotonda, F. Quaglia, Dry powders based on PLGA nanoparticles for pulmonary delivery of antibiotics: Modulation of encapsulation efficiency, release rate and lung deposition pattern by hydrophilic polymers, *Journal of Controlled Release* 157(1) (2012) 149-159.
- [99] M.S. Ural, M. Menéndez-Miranda, G. Salzano, J. Mathurin, E.N. Aybeke, A. Deniset-Besseau, A. Dazzi, M. Porcino, C. Martineau-Corcós, R. Gref, Compartmentalized Polymeric Nanoparticles Deliver Vancomycin in a pH-Responsive Manner, *Pharmaceutics* 13(12) (2021).

Biographical Information

Uday Kumar Chintapula was born and brought up in Hyderabad, India. After finishing high school, he joined Jawaharlal Nehru Technological University at Anantapur for his bachelor's degree in Biotechnology as a first-generation college student in his family. After completing 4 years, Uday applied to graduate school. During his master's program (MS), he worked on projects including synthesis of binary logic gates via chemically induced promoter switching in *E. coli*. and A-mode ultrasound registration of skull surface for computer-assisted surgeries, which was part of his MS thesis. Following completion of his master's degree, Uday joined UTA in 2016 as a doctoral student working in Dr. Samir Iqbal's lab as a rotation student where he worked on topics of single cell analysis and circulating tumor cells. Afterwards, Uday moved to nanomedicine and the tissue engineering laboratory in May 2018, where he worked on several projects related to nanoparticles as drug delivery systems. As a doctoral student, Uday received several awards such as the Dr. Franklyn Alexander scholarship for outstanding student and academic excellence, a STEM fellowship for graduate teaching and research assistant, and an I-engage mentoring fellowship. During his research career at UTA, Uday has published 5 research papers and 5 conference proceedings. Uday was highly active in academic affairs representing the bioengineering department for high school lab tours, a mentor program for helping new graduate students, an I-engage summer mentor for undergraduate student research, and as a graduate teaching assistant for several courses. Following his PhD, Uday plans to continue his research career in targeted drug delivery, tissue engineering, and synthetic biology inspired bioengineering.